AN ABSTRACT OF THE THESIS OF

Matthew R. MacDougall for the degree of Master of Science in Nuclear Engineering presented on June 23, 2015.

Title: Capabilities of Detecting Medical Isotope Facilities through Radioxenon Sampling

Abstract approved: _____

Andrew C. Klein

Medical Isotopes are a necessity in modern medicine for cancer treatments and medical imaging. In order to ensure that the needs and demands are met for the medical procedures, facilities are put in place to produce these isotopes. There are over 25 different isotopes of interest being produced by more than 35 research reactors across the United States. A key component in medical isotope production is the isotope separation process. During this process, several types of radioactive gases are released that would otherwise not leave the nuclear fuel component. One of these radioactive gases is radioxenon. The release of radioxenon into the environment is of concern to the Comprehensive Test Ban Treaty Organization (CTBTO) as one of the key critical sampling techniques utilized to detect a nuclear detonation is the presence of radioxenon. As more facilities release radioxenon, background levels increase, desensitizing the equipment, and making it more difficult to detect. For this purpose, the detection of a medical isotope facility through the use of radioxenon is an interest to the CTBTO as an attempt to reduce the background levels of radioxenon and ensure that the detonation capabilities remain unaffected. This thesis will investigate the capabilities of detecting these medical isotope facilities through the use of radioxenon detection. Additionally, probabilities of detection will be determined in order to accurately identify these facilities.

Capabilities of Detecting Medical Isotope Facilities through Radioxenon Sampling

by:
Matthew R. MacDougall

A THESIS

submitted to

Oregon State University

in partial fulfillment of
the requirements for the
degree of

Master of Science

Presented June 23, 2015
Commencement June, 2016

Masters of Science thesis of Matthew R. MacDougall presented on June 23, 2015.

APPROVED:

Major Professor, representing Nuclear Engineering

Head of the Department of Nuclear Engineering and Radiation Health Physics

---

Dean of the Graduate School

I understand that my thesis will become part of the permanent collection of Oregon State University libraries. My signature below authorizes release of the thesis to any reader upon request.

Matthew R. MacDougall, Author

ACKNOWLEDGEMENTS

The Author expresses sincere appreciation to all those that helped with the reviewing of this thesis. Specifically, Thomas Holschuh, Dr. Andrew Klein, Sean Kreyling, Katie McGivern, Alex Misner, Dr. Camille Palmer, Dr. Albert Stetz, and Dr. Haori Yang.

TABLE OF CONTENTS

TABLE OF CONTENTS (Continued)

LIST OF FIGURES

LIST OF FIGURES (Continued)

LIST OF TABLES

Dedication

This thesis is dedicated to the honor of Greg and Mary MacDougall. Without their love and support, this would have not been possible.

1. Introduction

Medical isotope facilities have become a necessity to modern medicine for procedures such as cancer treatment and imaging. Although these isotopes are a necessity, they pose an unsuspected issue to the detection of nuclear detonations. The radioxenon released through routine operations of these facilities is the same radioxenon isotopes used to monitor for a nuclear detonation by the Comprehensive Test Ban Treaty Organization (CTBTO). As the use of medical isotope facilities is only bound to increase, the detection of these facilities must be investigated. The purpose of this thesis is to investigate what the lowest release limits are for detection of a medical isotope facility through the sampling of xenon-133 and xenon-135. In order to do this, environmental conditions will be specified through a quasi-random number generation method called Monte-Carlo sampling. This will determine the environmental conditions, such as wind speed and direction, from a distribution obtained from the National Oceanic and Atmospheric Administration database. Applying these conditions to a Gaussian plume model will provide a plume to the selected conditions. This plume will then be applied to a spacial mesh and compared with existing detection limits for radioxenon. Then, by repeating the plume generation process several times, a total probability of detection will be calculated for the scenario. The ultimate goal of this thesis is to determine the detection limits through applying a threshold value and determine the maximum distance from which the facility can be properly detected. This will ensure proper and up to date knowledge of radioxenon emissions for application to CTBTO technology.

2. Literature Review

To support the modern peaceful use of nuclear technology, an investigation was performed to determine the relationship between nuclear science applications development and nuclear weapons proliferation in countries that participated in the original Atoms for Peace program [1]. This study concluded that there is an impact on both a weapons program from a peaceful use program and vice versa. The relationship between a weapons program and civilian power uses, as determined by the study, states that if a country is interested in creating a nuclear weapons program, it is likely to fail in creating a civilian nuclear power program, due to the fact that the

connection to the global economic market and international trade is diminished through the interest in a weapons program, since a high GDP per capita is a necessity for a civilian reactor program. Another study was performed in an attempt to evaluate the probability of countries' nuclear proliferation decisions [2]. In order to do this, several data points were taken in relation to the country. These data points included: economic status, security environment, political development, nuclear technological capability, and commitment to nuclear nonproliferation. However, some data points of interest are only available within a certain time period due to the implementation of new protocols (i.e. International Atomic Energy Agency Additional Protocol adopted in the 90s [3]). This study successfully quantifies the proliferation probability of each country that was investigated.

Further analysis can be conducted through the use of fuzzy logic and the probability that different nations will continue to act as a peaceful state. It has been determined when considering undetected nuclear activities; a nation under integrated safeguards can be maintained at very low proliferation risks [4]. An alternative view at proliferation attempts to reach the same conclusion by examining outsider threats. An outsider threat analysis is achieved through modeling and evaluation of proliferation resistance of nuclear energy systems. Furthermore, it is possible to quantify the risk or probability of proliferation resistance of a nuclear energy system (NES). Risk quantification is conducted through the development of Markov models for different proliferation resistant strategies. Two main situations considered are the covert/overt strategy as well as the NES operating with two different material flow modes: batch and continuous. A simple example consists of comparing a Canadian Deuterium Uranium (CANDU) reactor to a Light Water Reactor (LWR) [5]. The CANDU reactor has continuous material flow through the core (similar to the Hanford reactors during the Manhattan project), whereas the LWR loads many fresh fuel assemblies into the core during a complete reactor shutdown, operates, and then removes the spent fuel assemblies. The continuous loading poses a higher proliferation risk, and this study quantifies the risk and provides conclusions of the overall risk. The final study performs a critical analysis on advanced, Gen IV nuclear energy systems and their respective improvements with regard to strengthening nuclear non-proliferation and supporting nuclear disarmament. Specifically through converting nuclear weapon stockpile material into reactor fuel through the Mixed Oxide (MOX) project initiative and burning the resulting MOX fuel in reactor

cores [6]. These studies provide a relevant background to the current, global proliferation concerns. Furthermore, recognizing the potentially proliferated material (i.e. plutonium or uranium) when investigating a particular situation will help indicate what modes of material processing will be required and thus will provide investigators with appropriate context when searching for a material diversion or proliferation operations.

Of these different operations, the first process of interest is the Plutonium Uranium Redox Extraction (PUREX) operation [7]. The PUREX process originated from the Manhattan Project era when the extraction of plutonium was necessary for weapons production. Reports from as early as 1949 provides a very good overview of what capabilities are necessary for this type of operation [7]. The main chemicals of interest for separating the plutonium and uranium from fission products are tributyl phosphate (TBP) following dissolution of the fuel in nitric acid. A subsequent report from Oak Ridge National Lab (ORNL) provided an update on the metallurgical waste problems that originated with a PUREX pilot plant. [8]. Following this report, a construction project, overseen by Du Pont, of F-Area PUREX facilities was completed in the 1950's at the Savannah River Plant in Aiken, SC, which was capable of processing 10-13 MT of uranium per year [9].

Another case study pertaining to the PUREX process is the Uranium- Zirconium alloy fuel processing in the ORNL Volatility Pilot Plant [10]. This plant was originally meant to recover nuclear fuel material through a molten salt mixture to produce a uranium hexafluoride product for aircraft reactor experimental fuel. This plant was intended for fuel with a very low burn up (i.e. 100,000 gamma counts per mg of uranium) and was altered for zirconium-uranium alloy fuels in HF dissolution. This case study provides a unique perspective when examining the conversion of a facility repurposed for reprocessing operations. It represents the possibility for an operation to arise from a facility that originally claimed one use, and has been transformed for another. Reprocessing is becoming an increased topic of discussion because of the increased demand for electricity in the future and potential, proportional expansion of the use of nuclear power [11]. With an increased use of nuclear power, the demand for uranium will increase through natural economic progression and eventually, reprocessing will need to be considered from a cost-benefit analysis, rather than a uranium abundance analysis. Not only does

reprocessing increase the availability of uranium, but it addresses several environmental concerns for spent fuel management, thus increasing the sustainability of nuclear power [12]. For nuclear power to be a viable option in the future, it will have to become more prevalent and follow in the footsteps of France's La Hague plant (reprocessing facility used for commercial fuel) and embrace reprocessing operations. However, the diversion of material within a reprocessing plant is a large concern due to the abundance of fresh uranium fuel and plutonium separated as part of normal operations. For this reason, real time verification methods of accounting for Special Nuclear Material (SNM) are employed, which is possible through several methods, including the tensioned metastable fluid detector [13]. This particular technology performs well in extreme environments (large gamma and beta fluxes) and provides neutron spectroscopy, directionality, neutron multiplicity, and alpha spectroscopy with a very high intrinsic efficiency. However, concerns still exist due to the build-up of Am-241 and Cm-242. Similar to this project, the FIGARO project aims at detecting nuclear material through the use of high energy gamma rays (6-7 MeV) from the F-19 (p,$\alpha\gamma$) O-16 reaction [14]. With these high energy photons, the photo neutron and photo fission cross sections for isotopes that exist within SNM are high enough to allow for a potential interaction, thus enabling the ability to monitor waste streams through active Non-Destructive Assay (NDA) methods.

The cost of reprocessing is an additional concern from an economic standpoint. It was estimated in 1983 that a reprocessing plant able to process 1500 MT of Heavy Metal (MTHM) per year at 1.05 to 2.4 billion dollars with ~6% annual operating costs. The costs then increased by 50% (to ~9%) when considering fast reactor fuel [15], showing that reprocessing is not a trivial feat to accomplish and will leave significant administrative evidence beyond the chemical signatures from an operation point of view.

Another form of reprocessing besides the PUREX process is pyroprocessing. Pyroprocessing differs from the PUREX process in several ways. Pyroprocessing occurs at very high temperatures (~1200 °C) [16], and is preferred for its ability to extract uranium and plutonium from fuel in the form of metal as opposed to dissolving the fuel in a solution as is the case with the PUREX process. Historically, pyroprocessing has been employed at Idaho National Lab for the spent fuel from the Experimental Breeder Reactor (both I and II) which contains

significant amounts of zircaloy within the fuel, eliminating the possibility of the PUREX process [16].

Proliferation risks due to reprocessing not only come from commercial power reactor fuels, but can also come from research reactor fuel as well. Due to the higher uranium enrichment in research reactors (~20 wt% U-235) the global threat reduction initiative (GTRI) has implemented the use of U-Mo fuel [17]. The molybdenum in the fuel virtually eliminates the PUREX possibility for fuel.

With reprocessing being established as a valid concern, there have been several investigations to the radiological characteristics that result from these different reprocessing methods. During the extraction of any sort of spent fuel, releases of the radioactive noble gases are inevitable. For this reason, advance detection of noble gases has been an area of research pertaining to the detection of reprocessing. This has been done through Xe-133 and other noble gas monitoring at the Meteorological Research Institute, Tsukuba. The Meteorological Research Institute has been monitoring the levels of Xe-133 through atmospheric samples [18]. A characteristic isotope to sample for is Xe-133 with a half-life of 5.247 days due to the low reaction capabilities characteristic of noble gases. Background counting is a necessity when determining the Minimum Detectible Activity (MDA) and is a fundamental aspect to any experiment. This allows for technologies such as the atom trap trace analysis [19]to be conducted that will be able to process 1 liter of air within 3 hours.

Similar to reprocessing, uranium enrichment began back with the Manhattan project of WWII to supply increasing demand of highly enriched uranium (HEU) for weapons purposes [20]. To meet this demand, three main gaseous diffusion plants (GDP) located at Oak Ridge, Tennessee, Paducah, Kentucky, and Portsmouth, Ohio were constructed. Uranium enrichment advanced with the development of the Calutron, which was designed by Earnest Lawrence and functions through gaseous centrifuge technology. Similar to gaseous diffusion, the end goal was to separate the most abundant isotope of uranium, U-238, from the fissile isotope, U-235. The first calutron facility was built in Oak Ridge Tennessee and housed over a thousand calutrons during WWII to create the material used in Little Boy and enriched 50 kg of U-235 within one year of its construction [21]. Two levels of enrichment, alpha and beta, are meant to enrich the

material at two different stages, increasing the efficiency of the process. Since then, the uranium abundance has been split into 5 different periods based upon the demand for it [22]. These periods are: uranium ignorance, uranium positive control, uranium laissez-faire, uranium slip, and steady state uranium. All of these periods are a function of how uranium was treated and the associated actions the US took to manage the uranium. The handling of HEU for modern facilities is dictated by DOE Order 474.2- Nuclear Material Control and Accountability [23]. Nuclear Material Control and Accountability (MCA) is the concept of nuclear accounting and keeping track of all Accountable Nuclear Material (as defined by DOE O 474.2) at a site and ensure no material gets lost or unaccounted for. This DOE Order describes the establishment and maintenance of a Material Control and Accountability program. Each DOE site and facility operator needs to establish a sustainable graded safeguards program that is in compliance with this DOE Order to detect and deter theft and diversion, and to prevent the unauthorized control of a weapon, test device, or materials that can be used to make an improvised nuclear device. On a broader scope, understanding the capabilities of other countries enrichment capabilities is not only imperative to national security, but also to nonproliferation of military use of nuclear material. Of two most prevalent ways of enriching uranium, gaseous diffusion, which uses older technology and large amounts of power, or gas centrifuge separation, which uses advanced technology and is much more energy efficient. The current enrichment capacity of the world is 56 million kg seperative work units (SWU) per year. 22.5 million kg SWU in gaseous diffusion and more than 33 million kg SWU in gaseous centrifuge. The Uranium Enrichment Profile report provides a snapshot overview of the world enrichment capacity in 2009 and provides uranium enrichment programs of individual states. [24]. The enrichment capabilities of countries will inevitably increase the proliferation risk and thus provide an increased interest during the policy study. The enrichment portfolio is of interest to understand the justification behind the two modes of enrichment and will support the detection of the enrichment aspect in understanding what the characteristics are of the different enrichment types. Looking forward, the future of uranium enrichment concepts of chemical enrichment using ion exchange (redox) is being considered [25]. The proliferation risk of an enrichment facility using this methodology has a unique capability that prevents the enrichment of uranium past 50% U-235, which is accomplished through controlling the multiplication factor, or k value, of the material

configuration throughout the enrichment facility. As one enriches the material past 50% U-235, the configuration of the material will cause the multiplication factor of the assembly to approach unity, causing the enrichment facility configuration to go critical. Furthermore, the time required to enrich from 50% to 90% U-235 will require ten thousand days of additional operation, making it nearly impossible to get weapons-grade uranium from the redox ion exchange method.

With new and modern technology for enriching and reprocessing nuclear material, advanced detection methods are coming forth to identify smaller quantities of material characteristic to discovering material operations. The two primary assay modes used to detect SNM are active and passive. Passive NDA utilizes natural properties of the material, either radioactive or otherwise, to determine the type of material within the sample. Active NDA induces a reaction in the sample material with the use of particles being shot at a material (either neutron or photon) and observing the material response. Active detection can be very useful when dealing with special nuclear materials as the properties of interest are in fact the response to these interstitial particles.

Passive measurement can be preferred in some situations, since the equipment required is much lighter and typically provides a lower dose to the user than active measurement [26]. The Pa-234m 1.001 MeV Gamma is a good indicator of U-238. About 100 gammas per second per gram of U-238 are to be expected for this measurement. However, this method can be unstable in an aqueous environment due to uranium accumulation though it can be a very good baseline for detection. In order to verify this technique, sediment samples are investigated through gamma spectroscopy. The results are portrayed in real time, making this method of verification convenient for in-situ measurements. Furthermore, through natural decay calculations, one can determine if the sample obtained is in secular equilibrium with natural material (i.e. expected background radiation levels and ratios). Secular equilibrium is verified through analysis of the thorium and uranium decay series with low-energy gamma rays spectroscopy. Some isotopes of interest are: Ac-228 and Pb-212 for the thorium series, and Pa-234, Ra-226, and Bi-214 for the uranium series. [27]. Through experiments similar to this, secular equilibrium condition may be tested for the thorium series, however, this relationship is not valid for the uranium series where

disequilibrium, a common occurrence in water-lain series. Documents providing the expected ratios for isotopes of interest are helpful in determining the mass specific activity of isotopes that would indicate an increased amount in either the thorium or uranium decay series, which is of interest in order to detect uranium enrichment [28]. If sampling directly for the actinide decay chain is not desired, sampling for U-235 directly is possible through multi-group gamma-ray analysis. Multi-group gamma-ray analysis method for uranium (MGAU) was used as a nondestructive assay method applied to certified reference nuclear materials containing 0.32-4.51 at% U-235. MGAU provides incorrect results for materials containing low concentrations of U-235, found in the tailings of uranium enrichment or depleted uranium because the build-up of decay products [29]. However, it is possible to account for these discrepancies when running advanced simulations to anticipate these build ups. All of the discussed methods are applicable to the IAEA for verifications of uranium enrichment plants of Non-Proliferation Treaty (NPT) member states [30].

Medical isotope facilities produce material necessary for modern medicine. However, the radiation released from these facilities cause issues that are non-health related and pertain to detection of nuclear weapons, allowing inspectors to ensure that total compliance with the Comprehensive Test Ban Treaty (CTBT) is met by all States. As enforced by the Comprehensive Test Ban Treaty Organization (CTBTO), the first two statements of the CTBT preamble summarize the significance of the treaty as an important nuclear non-proliferation and disarmament measure [31]. This treaty elaborates upon the Partial Test Ban Treaty (PTBT), which put a stop to all atmospheric, underwater, and outer space nuclear weapon testing due to radiation dispersal concerns. The PTBT however, did not address underground testing of nuclear weapons and, as a result, countries moved to underground testing to progress their respective weapons program [31]. The CTBT encompasses the PTBT, and additionally eradicates underground testing which, in effect, eliminates all possibilities of nuclear weapons testing. In order to enforce this treaty, the CTBTO currently has 337 publicly acknowledged stations that utilize seismic, hydroacoustic, infrasound, and airborne radionuclide sensors that monitor for characteristics of a nuclear weapon detonation [31]. The monitoring mode of interest is the radionuclide detection systems that sample for particulate as well as radioactive noble gases,

specifically radioxenon. Medical isotope facilities produce large amounts of radioxenon in their regular operation, which causes issues for the International Monitoring Stations (IMS) since these stations rely heavily on low background levels of radioxenon to ensure accurate and precise detection of a nuclear detonation [32]. Medical isotope production facilities can release a range of $10^9 to\ 10^{13}$Bq/day, though validated calculations indicate emissions in the range of $5 * 10^9$ as acceptable and within the realm of possibility [32]. Additional studies conducted at Pacific Northwest National Labs (PNNL) have been performed pertaining to the detection of transuranic waste buried underground in the 200 Area West. Samples taken in this area were in excess of 10^5 Bq, but when investigating the limits of detection, or MDA, it was determined that the equipment was capable of detecting $0.5\frac{mBq}{m^3}\ and\ 3.0\frac{mBq}{m^3}$ for xenon-133 and xenon-135, respectively [33]. Both these data values (source strength and MDA levels) are imperative when considering the simulation of xenon transport and detection.

Detection of reprocessing is more convenient since the characteristics are much easier to detect due to the increased radioactivity associated with the process, focusing on four main areas: remote sensing for nuclear safeguards, proliferation indicators, measurements technologies, safeguards procedures. The remote sensing for nuclear safeguards focuses specifically on the reprocessing facilities for plutonium processing capabilities. The second section, proliferation indicators, focuses on the isotopes that indicate material separation processes: Xe-131 and I-129 as atmospheric samples, U-236 in aqueous effluents or aerosol particles, and TBP in aqueous effluents. The measurement technologies section discusses different sampling techniques that will allow the IAEA or other enforcing agencies to detect the releases discussed in section 2 [34]. Lastly, the safeguards procedures discuss different enforcing procedures put in place by the IAEA and their applications.

1. Medical Isotope Production Overview

Specific isotopes have been identified for use in the medical industry for imaging as well as treatments. As modern medicine has developed, the demand for medical isotopes has increased as well, and for this reason, medical isotope production facilities are becoming more prominent

across the globe. However, because medical isotope facilities are a necessity for modern technologies in the medical field, they pose a significant and increasing problem for the Comprehensive Test Ban Treaty Organization (CTBTO). Radioxenon is a very good indicator that a nuclear explosion has occurred as it is a common fission product produced through ^{239}Pu and ^{235}U fission, but this same radioxenon is produced through the material production and processing at a medical isotope facility. Radioxenon is desirable because it is a noble gas, making it difficult to conceal activities in a facility due to the low probability of capture prior to its release in the free atmosphere [35].

1.1. Facility Types

There are two main facility types when considering medical isotope production: isotope production reactors and particle accelerators, and these facilities are of interest when considering the capabilities to meet the demand for medical isotopes. Medical isotope facilities function under the observation of the Nuclear Regulatory Commission (NRC), and as a result, these facilities are responsible for observing the safeguards and securities put in place by the NRC to ensure that all nuclear materials are properly guarded and accounted for.

1.1.1. Medical Isotope Production Reactors

Isotope production reactors are utilized for the abundance of free neutrons that cause neutron interaction transmutations. For example, the production of ^{99m} Tc uses the neutrons to induce transmutation of 98Mo to ^{99}Mo with subsequent beta decay to ^{99m}Tc. Due to the short half-life of molybdenum-99 stockpiling is not an option [30]. Although this method is feasible, it typically not what is implemented as Mo-99 production through U-235 targets proves to be much more efficient [36]. In the past, highly enriched uranium (HEU) targets have been utilized for this process but, due to the current safeguard and nonproliferation culture, recent studies are investigating the feasibility of producing the same amount of Mo-99 but with low enriched uranium (LEU). The processing of ^{235}U targets is the source of the radioxenon from these facilities and what causes concern by the CTBTO. In addition to medical isotopes, fission products can be useful in some other applications of nuclear technologies. The radioisotope Cs-137, for example, is a another common fission production of thermal ^{235}U fission [36], is

produced at the High-Flux Isotope Reactor (HFIR), operated by Oak Ridge National Laboratory (ORNL) for the Department of Energy (DOE). The reactor has a nominal power level of 85 MW and is fueled by highly enriched uranium fuel elements. This highly enriched fuel produces a very large neutron flux of $4 * 10^{15} \frac{neutrons}{cm^2 s^2}$, and is capable of doing 26-day irradiation cycles. Some common isotopes produced in HFIR are: ^{75}Se, ^{252}Cf, ^{188}W/^{188}Re, and ^{63}Ni. A similar facility is the Advanced Test Reactor (ATR) located at Idaho National Labs (INL). This reactor does not produce the same neutron flux or the diverse portfolio of isotopes. Instead, it functions at a neutron flux of $4 * 10^{14} \frac{neutrons}{cm^2 s^2}$ and produces mainly ^{60}Co. Other reactors include: National Research Universal at Chalk River, Ontario, Brookhaven Linac Isotope Produce at Long Island, NY, and the Isotope Production Facility at Los Alamos, NM.[36]. These facilities can release a range of $10^9 to\ 10^{13}$Bq/day, though calculations performed and validated indicate emissions in the range of $5 * 10^9$ as acceptable and within the realm of possibility [32].

From a nonproliferation standpoint, medical isotope reactors pose a very difficult situation as the irradiation and material separation process for the isotopes can closely resemble a process utilized for plutonium production. The target loading and unloading times will vary as a function of the desired medical isotope and will typically range on the order of months irradiated in the reactor. For example, in the production of iodine-131, the desired loading and unloading time is approximately 55-60 days [37]. This same irradiation time when considering targets used for plutonium production will yield >%96 ^{239}Pu isotopic purity per unit mass [37]. On site investigations conducted by the IAEA ensure that the facilities utilizing a medical isotope production reactor function to produce the declared isotope and the facilities are not used for the production of special nuclear material. Furthermore, the chemical separation process is drastically different between medical isotopes and ^{239}Pu, which provides significant evidence for the frequent and routine investigations performed to ensure this situation, is not occurring.

1.1.2. Particle Accelerators

The second medical isotope production facility type is a particle accelerator. Worldwide, there are currently 200 particle accelerators that are utilized for medical isotope production [38]. The first particle accelerator was utilized to understand how the atomic nucleus functioned and

was utilized to bombard lithium targets with protons to produce two Helium nuclei by Corkroft and Walton in 1932[38]. Modern accelerators function on the same property as this reaction: accelerating a charge particle (light or heavy) at a target to transmute it to a different daughter product.

As the particle accelerators have evolved over the years, different types of particle accelerators have been developed to function specifically designed for the desired objective. The first type of particle accelerator of interest is the Potential-Drop Accelerator (PDA), which is the most basic type and was utilized for the early particle accelerators. In the PDA design, the potential difference between an anode and a cathode and accelerates the charged particle across the difference using static DC power as depicted in Figure 1. The highest recorded difference is 20 MV, which accelerates an electron up to energy of 20 MeV [38]. The Daresbury Lab, located in the United Kingdom, utilizes this type of technology.

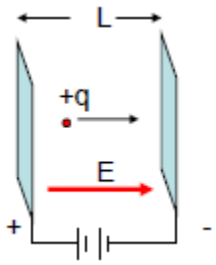

Figure 1: Potential Drop Accelerator

The next type of particle accelerator energizes particles by repeated application of time-varying acceleration field, and can function in two main orientations: circular or linear. The circular accelerator will utilize specially orientated radio-frequency accelerators that, as the particle travels the pathway, will accelerate the particle until it has reached the desired kinetic energy as depicted in Figure 2 [38]. This orientation can be convenient to conserve materials as the particle's path is repeatedly used until the particle reaches very high energies. Cyclotrons used for nuclear material production employ this technique. The second orientation type as depicted in Figure 3 is the linear accelerators which utilize the path length and acceleration cavities once through to accelerate the particle to the desired kinetic energy [38]. This orientation is desired for small scale experiments that accelerate a particle to a lower energy when compared with the circular orientation. This orientation is utilized in x-ray technology in the acceleration of

a beam of electrons to a tungsten target, with the resulting collisions producing Bremsstrahlung photons used for the imaging process. As these facilities do not utilize fission based isotope production, there is no release of radioxenon through the facility operation and thus will not be included in further analysis of the thesis.

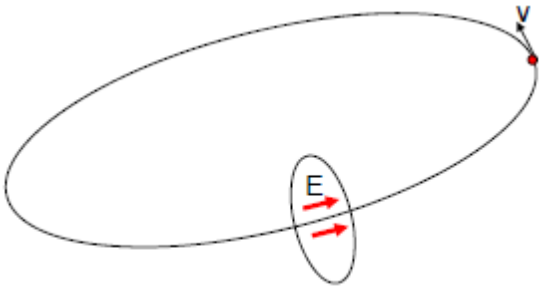

Figure 2: Circular accelerator orientation through time-varying accelerating fields [38]

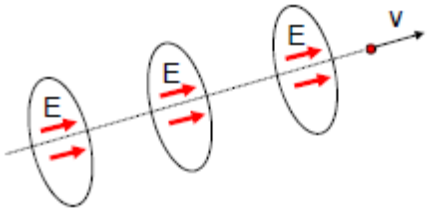

Figure 3: Linear accelerator orientation through time-varying accelerating fields [38]

2. Reprocessing

Medical isotope separation and reprocessing of spent nuclear fuel are both ways of separating desired isotope from all other nuclear material, with the main difference being the desired material after separation. As previously mentioned, this could be considered a viable way to convert peaceful uses of nuclear technology to militarized uses, and further investigation is needed to understand what differences occur in the separation process, which encompasses the unused nuclear fuel (i.e. uranium and plutonium) from nuclear waste (i.e. fission products). This method is typically discussed when uranium and/or plutonium are retrieved from spent nuclear fuel from power or research reactors or from depleted uranium targets placed in a high flux reactor. Separation of uranium and plutonium for a closed fuel cycle is the same process desired for the foundation of a weapons complex, thus establishing the foundation of proliferation risks. When considering the isolation of special nuclear material from other material, there are limits for both uranium and plutonium. These limits are dictated by the isotopic purity and are established within DOE Order 474.2- Nuclear Material Control and Accountability [23]. For uranium, an assay of 93% uranium-235 is considered to be weapons grade material. For

plutonium, an assay of 92% plutonium-239, and at most, 8% plutonium-240 is considered ‘weapons grade material’ [7]. Figure 4shows a flow chart of material attractiveness.

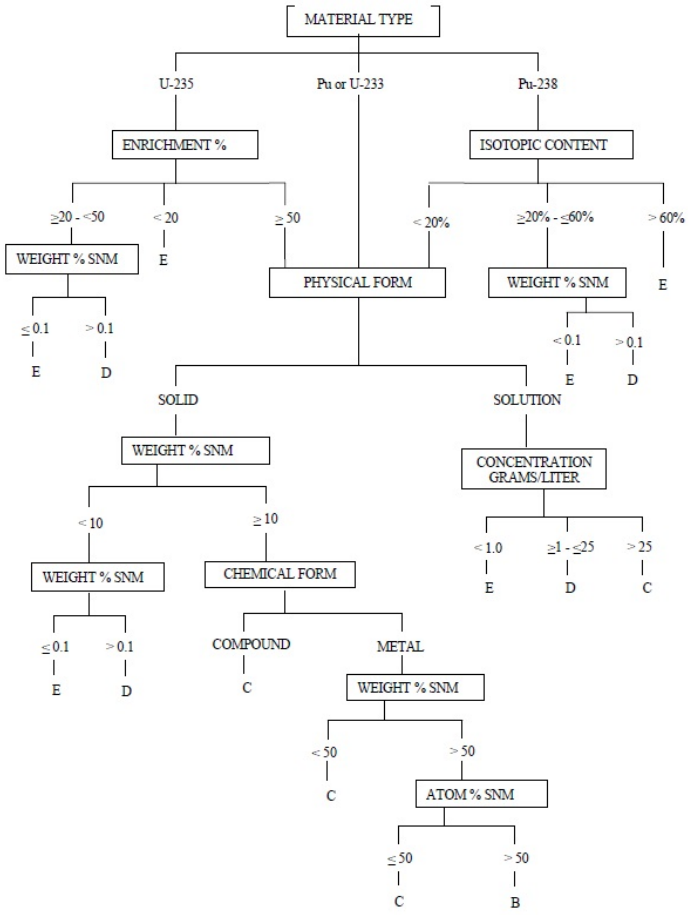

Figure 4: Material Attractiveness Flow Chart [23]

The Material Attractiveness definitions are as follows:

A. Attractiveness Level A: Weapons and test devices; partially assembled weapons and test devices sufficient to construct an improvised nuclear device using commercially available parts and materials.

B. Attractiveness Level B: Pure forms of SNM with a total SNM content exceeding 50 atom percent; that is, greater than half of the atoms present in the material must be SNM. The SNM can be used in its existing form, or that can be utilized after simple mechanical removal of cladding, packaging, or matrix material to produce a weapon/improvised nuclear device through casting, forming, or other nonchemical operations.
C. Attractiveness Level C: High-grade SNM that can be easily converted to metal. Generally, these materials are of high purity and require relatively little processing time or effort to obtain Level B material.
D. Attractiveness Level D: Low-grade SNM that are more dilute or of lower purity than Level C materials, and require greater processing time or greater processing complexity to convert to metal than Level C materials.
E. Attractiveness Level E: All accountable nuclear materials that do not meet the criteria for Attractiveness Level A through D.

Two definitions of terms are required to understand the attractiveness levels. These terms are "Special Nuclear Material" and "Accountable Nuclear Material".

- Special Nuclear Material is defined as "Plutonium, uranium-233, uranium enriched in the isotope 235, and any other material, which pursuant to 42 U.S.C. 2071 (Section 51, as amended, of the Atomic Energy Act of 1954), has been determined to be special nuclear material, but does not include source material; or any material artificially enriched by any of the forgoing, not including source material."
- Accountable Nuclear Material is defined as "Nuclear materials as defined in DOE M 470.4-6, Nuclear Material Control and Accountability, Table I-1." Table I-1 can be found as Table 1.[23]

Table 1: Table I-1 from DOE M 470.4-6 [23]

Material Type	SNM, Source, or Other	Reportable Quantity*	Weight Field Used for Element	Weight Field Used for Isotope	Material Type Code

Depleted Uranium (U)	source	kilogram	total U	U-235	10
Enriched Uranium	SNM	gram	total U	U-235	20
Normal Uranium	source	kilogram	total U	—	81
Uranium-233	SNM	gram	total U	U-233	70
Plutonium-242[1] (Pu)	SNM	gram	total Pu	Pu-242	40
Plutonium-239-241	SNM	gram	total Pu	Pu-239 + Pu-241	50
Plutonium-238[2]	SNM	tenth of a gram	total Pu	Pu-238	83
Americium241[3] (Am)	other	gram	total Am	Am-241	44
Americium-243[3]	other	gram	total Am	Am-243	45
Berkelium[6] (Bk)	other	microgram	—	Bk-249	47
Californium-252 (Cf)	other	microgram	—	Cf-252	48
Curium (Cm)	other	gram	total Cm	Cm-246	46
Deuterium[4] (D)	other	tenth of a kilogram	D_2O	D_2	86
Enriched Lithium (Li)	other	kilogram	total Li	Li-6	60
Neptunium-237 (Np)[3]	other	gram	total Np	—	82
Thorium (Th)	source	kilogram	total Th	—	88
Tritium[5] (H-3)	other	gram	total H-3	—	87
Uranium in Cascades	SNM	gram	total U	U-235	89

A reportable quantity is the minimum amount of material subject to the requirements of this manual. Facilities with less than a reportable quantity of a material are exempt from the requirements of the manual for that material. Facilities with more than reportable quantities are to report transactions that exceed a reporting unit or more of material, where a reporting

unit is defined as the mass unit that facility/site nuclear materials accounting systems must use for recording and reporting inventories and transactions. The superscripts in Table 1 are given as follows: [1]Report as Pu-242 if the contained Pu-242 is 20 percent or greater of total plutonium by weight; otherwise, report as Pu-239-241; [2]Report as Pu-238 if the contained Pu-238 is 10 percent or greater of total plutonium by weight; otherwise, report as Pu-239-241; [3]Americium and Neptunium-237 contained in plutonium as part of the natural in-growth process are not required to be accounted for or reported until separated from the plutonium; [4]For deuterium in the form of heavy water, both the element and isotope weight fields will be used; otherwise, report isotope weight only; [5]Tritium contained in water (H2O or D2O) used as a moderator in a nuclear reactor is not an accountable material; [6]Berkelium must be accounted for at the site level. It is not required that it be reported to the Nuclear Material Management Safeguard Software (NMMSS).[23]

2.1. Origin of material (Diversion Scenarios)

The reprocessing of nuclear material does not irradiate the material, but rather deals with the separation of already irradiated material. This requires that the material be irradiated at a different location and then diverted from that facility, an activity which the IAEA and DOE is constantly monitoring for through rigorous safeguards and securities. Isotopes of interest include U-235 and Pu-239; however, these nuclides are not abundant in nature (U-235 with 0.7% abundance in uranium ore [20]) or do not occur naturally (Pu-239) and therefore need to be manufactured. Pu-239 is created through the irradiation of natural or depleted uranium targets, which are mostly composed of uranium-238. Through neutron absorption and two subsequent beta decays, Pu-239 is formed.

U-235 is created through a process called uranium enrichment, where U-235 is extracted from natural uranium ore and separated. In this paper, the source material of concern will be irradiated targets or fuel and the diversions scenarios will pertain to nuclear reactors (either power or research). Diversion of material from enrichment is a possibility and will be considered

as processing scenario. However, for the purpose of this analysis, the diversion of HEU from an already declared scenario would not yield the source that is required for plume analysis.

In any given diversion scenario, there are two categories to consider: with or without the facility knowing of the diversion. The most important difference is the concept of safeguards. The primary role of safeguards is to deter the proliferation of nuclear weapons or nuclear material. This is demonstrated through no misuse of nuclear material or technology is being conducted that would lead to proliferation or a weapon development program [23]. From an international standpoint, the International Atomic Energy Agency (IAEA) provides the main oversight for safeguards at foreign and domestic research and power reactors. Their ultimate goal is to verify the correctness and completeness of nuclear material and technology use declarations made by the state, which is performed by employing different safeguards and security checks placed throughout the process of operating a nuclear reactor.

Since safeguards are a credible deterrent from the misuse of nuclear material, diversion activities subverting the facility's safeguards would need to be conducted in order for the material to become available for additional processing. Due to the isotopic content required for plutonium production, there is a scenario where plutonium targets will be irradiated and then extracted from the reactor core for processing. These targets will have a high concentration of U-238 and could include either natural or depleted uranium. However, inserting and removing specific targets from the reactor will have very noticeable impacts on power levels, neutron flux, and burn up of the fuel in the reactor, and these impacts are all accounted for by nuclear safeguards.

The next diversion scenario to consider is from the facility waste streams. Small quantities of accountable nuclear material within wastes streams are considered as material unaccounted for (MUF). MUF can also be inventory differences, which is the difference between the physical and administrative inventories [23], which may arise can occur from several different circumstances:

- Accumulation of uncertainties in measurement systems
- Human error in data entry
- Unmeasured items in the inventory

- Unmeasured or unaccounted for changes (i.e. decay)
- Theft
- Diversion of the material

Differences in the physical and administrative inventories are more common within processing facilities where nuclear material changes form, but can also occur in a reactor setting. Due to the uncertainties of NDA techniques on trace amounts, it is very possible for quantities to accumulate over time. Physical security measures are put in place to ensure proper safeguards of all forms of accountable nuclear material to avoid differences in inventories.

2.2. PUREX Process

The concept of extracting useful material from spent nuclear fuel is not a novel idea. In fact the first concept of PUREX originated was in 1949 at Oak Ridge National Lab with the idea of extracting uranium and plutonium to use for the manufacturing of nuclear weapons [7]. The two important chemicals pertaining to the PUREX process is TBP, an organic compound used for the separation of higher atomic weight actinides from lower atomic weight fission products, and nitric acid, a necessary in dissolving fuel rod assemblies to ensure that all materials are in an aqueous state.

Additional investigations into the PUREX process were conducted in the 1950s by ORNL in an attempt to modify the process to increase the efficiency at the Hanford plant in Richland, WA. Further investigations to the PUREX process placed emphasis in development of processing techniques, simplicity, cost, and the agility of future PUREX operations [8].

The following are the major steps of the PUREX process:

1. Transfer of irradiated targets or slugs from reactor to hot cell
2. Placement of targets into nitric acid dissolving tanks
3. Filtration of dissolver to remove any remaining solvents
4. Chemical treatment of the solution to ensure the proper valence state of the uranium and plutonium

5. Extraction of the uranium and plutonium through centrifugal section of the solvent extraction cycle
6. Separation of the plutonium from the uranium by the addition of TBP to the solvent
7. Addition of ferrous sulfamate to the solution to reduce plutonium's valence state and allows the change from solvent phase to aqueous phase
8. Purification of the plutonium stream; wash with fresh solvent to ensure proper separation of uranium from plutonium

After this process, this will fully enable the uranium and plutonium to be extracted from the solution and prepared for its final intended use. An example of a post processing is the creation of MOX fuel, manufactured at facilities such as the La Hague Plant in France, operated by Areva, which treats fuel obtained from several countries such as France, Japan, Germany, Belgium, Switzerland, Italy, Spain, and the Netherlands [39] [9].

2.3. Pyroprocessing

Pyroprocessing is a second method used to extract uranium and plutonium from nuclear fuel and targets. This process originated from the need to extract material from fuel used in the Experimental Breeder Reactor I, a sodium-cooled fast reactor located at Idaho National Laboratory. However, this process allows conversion of fuel waste directly into metallic form (typically of interest from a weapons standpoint). The metallic form of waste provides more options when considering long term disposal of nuclear material. Pyroprocessing provides a unique way to extract the plutonium and uranium from fuel that would otherwise be impractical with the PUREX process and avoids the use of harsh nitric acid solutions. Furthermore, from a detection standpoint, the amount of energy required to have this process function at 1200 ℃ and 0 kPa, would create a very large temperature signature (similar to gaseous diffusion plants in uranium enrichment) and would enable the detection to be more easily recognizable. [40] Figure 5 shows a generic flow chart for Pyroprocessing.

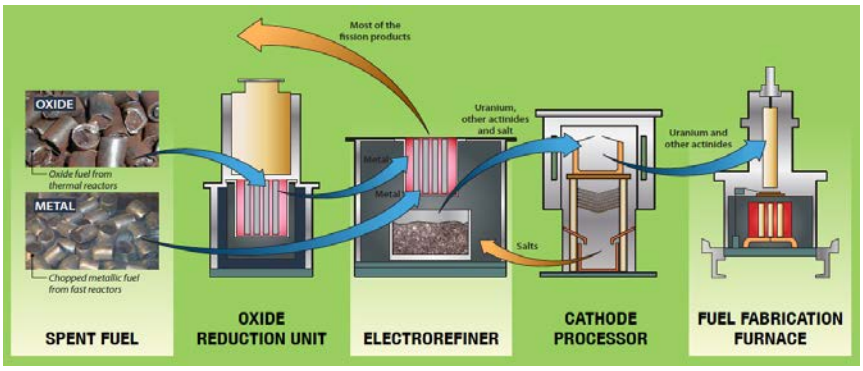

Figure 5: Pyroprocessing Flow Chart [41]

The critical component when considering pyroprocessing is the electrorefiner. The electrorefiner is a tool that is used for electrolytically separating uranium from cladding, coolant (sodium in this case), and other materials that have accumulated within the spent fuel. The components of an electrorefiner consist of an anode (basket) and two separate cathodes. The two cathodes differ in their composition: one is stainless steel and the other is a pool of liquid cadmium. While retaining the zirconium and other metallic fission products, the remainder of the fuel is dissolved. Separation occurs as uranium migrates to the first cathode and plutonium migrates to the second cathode, while the remaining solution consists of alkali and alkaline earth metals, with the noble metals falling to the bottom of the vessel [17][11].

Continuing the process, uranium is then coated with chloride and other salts until the mixture consists of 20 wt% of the product. Then, material is inserted into the cathode processor where the temperature is 1200 ℃ and the pressure is near 0 kPa. It is possible for plutonium to be separated using a similar technique from the second cathode.

2.4. Signatures of Reprocessing

Ultimately, when investigating the different extraction methods, the materials used are very unique to the process itself and thus, sampling for these very unique materials can be a very good indicator of material processing being conducted. Furthermore, this will aid in the detection of the processing of nuclear waste through both chemical and radiological releases.

When considering the both PUREX and Pyroprocessing, a very unique release of radioisotopes, specifically radioxenon (^{131m}Xe, ^{133}Xe, ^{133m}Xe, ^{135}Xe), will emerge from the

plutonium stream. These isotopes correlate very closely with the releases from a medical isotope facility and thus the exact origin of these radioactive noble gases from an unexpected source need to be treated with the utmost concern. Furthermore, the released isotopes will provide an excellent indication of the fuel itself since the compositions will be directly proportional to the exact compositions that were originally contained within the fuel. Through the use of burn-up codes such as MCNPX [42], one can determine the exact compositions in the fuel given the irradiation time and declared power levels [11].

The chemical signatures of the PUREX process are just as unique as the radiological releases. As described in the previous section, the PUREX process requires specific, identifiable chemicals that ensure the proper dissolution of spent fuel and extraction of plutonium and uranium, including nitric acid, sulfuric acid, sodium hydroxide, and sodium nitrate. Detection of these chemicals would not provide real time results due to necessary off-site laboratory techniques to verify the chemicals within the samples, but still can be used as a verification technique to radiological release sampling [9]. The chemical signatures of Pyroprocessing differ from the PUREX process; for example, pyroprocessing doesn't use the nitric acid used in the PUREX process. Additionally, the unique salts that are passed between the electrorefiner and cathode processor are not present in the PUREX process, and the extreme temperatures in pyroprocessing are good indicators of the processes taking place since the operating temperatures are well beyond 25 times that of the ambient temperature [41].

3. Relevant Treaties and Agencies

The applicable information for this thesis goes well beyond the technical aspect of detecting nuclear facilities. Treaties and regulations that mandate the verification of declared activities and the detection of separation activities are equally important. Section 3 will aim to discuss all of the treaties that impact nuclear nonproliferation from both a detection and verification standpoint.

3.1. Comprehensive Test Ban Treaty Organization

The Comprehensive Test Ban Treaty Organization (CTBTO) functions under the Comprehensive Test Ban Treaty (CTBT) that was established to ensure no more nuclear explosive devices were tested to initiate, develop, or expand a nuclear weapons program. The history of nuclear weapons testing has a long history prior to the establishment of the CTBT in 1996. Beginning with the Trinity test at Alamogordo, NM in 1945, nuclear weapons testing has been conducted across the globe. The first expression of concern pertaining to nuclear weapons testing was from Jawaharlal Nehru, Prime Minister of India that suggested a "standstill agreement" on nuclear testing [31]. Then, in 1963, the Partial Test Ban Treaty was created. Due to rising concerns of radioactive fallout occurring from high-yield thermonuclear testing, the Partial Test Ban Treaty was put in place to eliminate nuclear testing occurring in outer space, the atmosphere, and underwater. This treaty did not include any mention to underground nuclear testing. Following this event, the Nuclear Non-Proliferation Treaty of 1968, discussed in detail in Section 3.2. Following these milestones and the establishment of the Group of Scientific Experts, the United Nations Conference on Disarmament in Geneva in 1994, formal negations were initiated on the banning of all nuclear weapons testing. These negotiations lasted until 1996 and culminated in the establishment of the CTBT, which was signed by the initial 44 States (listed in Annex 2 of the CTBT). The list of initial states was formed by mandating that participating nations must have nuclear power or research reactor capabilities at the time of the CTBT's creation [31].

As stated by the basic obligations, "Each State Party undertakes not to carry out any nuclear weapon test explosion or any other nuclear explosion, and to prohibit and prevent any such nuclear explosion at any place under its jurisdiction or control [31]." The second point elaborates on the first by stating "Each State Party undertakes, furthermore, to refrain from causing, encouraging, or in any way participating in the carrying out of any nuclear weapon test explosion or any other nuclear explosion [31]."

The CTBT is enforced through the use of 337 International Monitoring Systems (IMS) that function on several sampling techniques. The first of these sampling techniques is the seismic monitoring technology used to detect an underground nuclear test, and is the largest

sampling network utilized by the CTBTO, consisting of 170 monitoring stations. These monitoring stations utilize seismometers in arrays that detect seismic activity in the earth's crust that would indicate activity indicative of an underground test [31]. The next monitoring type, hydroacoustic monitoring, is similar to seismic activity monitoring, but instead of detects waves propagating through the ocean water that would be indicative of a nuclear test. This sampling method utilizes 11 sampling stations across the world to properly monitor the oceans across the globe [31]. Next, infrasound monitoring samples the atmosphere for infrasound waves that would indicate a nuclear test, with sixteen of these station types currently implemented across the globe. These stations sample for sound waves that are inaudible to the human ear and are characteristic to very large scale events, such as a nuclear weapons test [31]. The last, and most important, technology to this study is radionuclide monitoring. Currently, 80 stations are implemented across the globe that sample for radionuclides and particulate characteristic of a nuclear event. These stations function through the use of air filters (for particulate) and continuous air flow detectors (for noble gases). The most important sampling isotopes are the noble gases that will easily escape an underground nuclear test, most notably the radioxenon nuclides (^{131m}Xe, ^{133}Xe, ^{133m}Xe, and ^{135}Xe) [43]. Figure 6 shows all of the publicly acknowledged IMS stations across the globe and Figure 7 shows the radionuclide stations within the IMS. Currently, the desire to reduce the amount of radioxenon has been an internationally collaborative effort in order to provide more accurate results for the IMS. Radioxenon is a byproduct of the medical isotope production and separation and releases into the environment is undesirable for this reason. In addition to the passive monitoring, on-site inspections are conducted to ensure that the development or research into nuclear weapons is not being conducted [31]. These stations compare the concentrations of the previously mentioned radioxenon isotopes and the ratios of ^{133m}Xe to ^{131m}Xe and ^{135}Xe to ^{133}Xe.

Through the comparison of these isotopes, it is possible to distinguish a possible nuclear explosion from regular power reactor operations and medical isotope production facilities. Figure 8 shows the comparison of these two ratios and the resulting radioxenon release source [44]. Figure 8 shows three separate regions of interest. The first region is reactor operations and is represented on the far left of the scale. The reason this section is so far away from the medical isotope production region of the figure is because fuel processing is usually not being conducted

at these power production sites. Therefore, the releases of radioxenon are far less and predominantly occur through fuel rod failures, which in today's nuclear industry is a rare occurrence. The next region of interest is medical isotope production and occurs very close to a possible nuclear explosion. This region has two features that require elaboration. The first is the narrow characteristic this region is in comparison with the other two regions. This is a result of the large amount of radioxenon filtration and trapping that occurs within the facility itself. This filtration is very important to reduce the background levels of radioxenon as well as providing this capability to distinguish between a possible nuclear explosion. The next main feature is how close it occurs to the possible nuclear explosion. This is because when the fuel is processed at these facilities, the radioxenon released is created through the same process in which the radioxenon from a nuclear detonation is created, namely the fission process. The last region of interest is the possible nuclear explosion and occurs to the far right of the graph. This region is very wide when comparing it to medical isotope production and this is due to the lack of radioxenon filtration and trapping. When an atmospheric nuclear detonation occurs, it is impossible to capture all of the radioxenon gasses released through the detonation process and results in a wide range of ratios for the radioxenon isotopes. However, in an underground nuclear weapon test, a very significant portion of the radioxenon produced is contained underground. Although in it is in trace amounts, some portion of the radioxenon is released to the atmosphere. The detection of this trace amount is of the utmost importance and supports the need to keep radioxenon background levels low and support the functionality of CTBTO technology. Furthermore, the ratios of radioxenon released from the explosion are largely a function of the device itself. Therefore, different device types that utilize different materials will release very different radioxenon ratios when compared with one another.

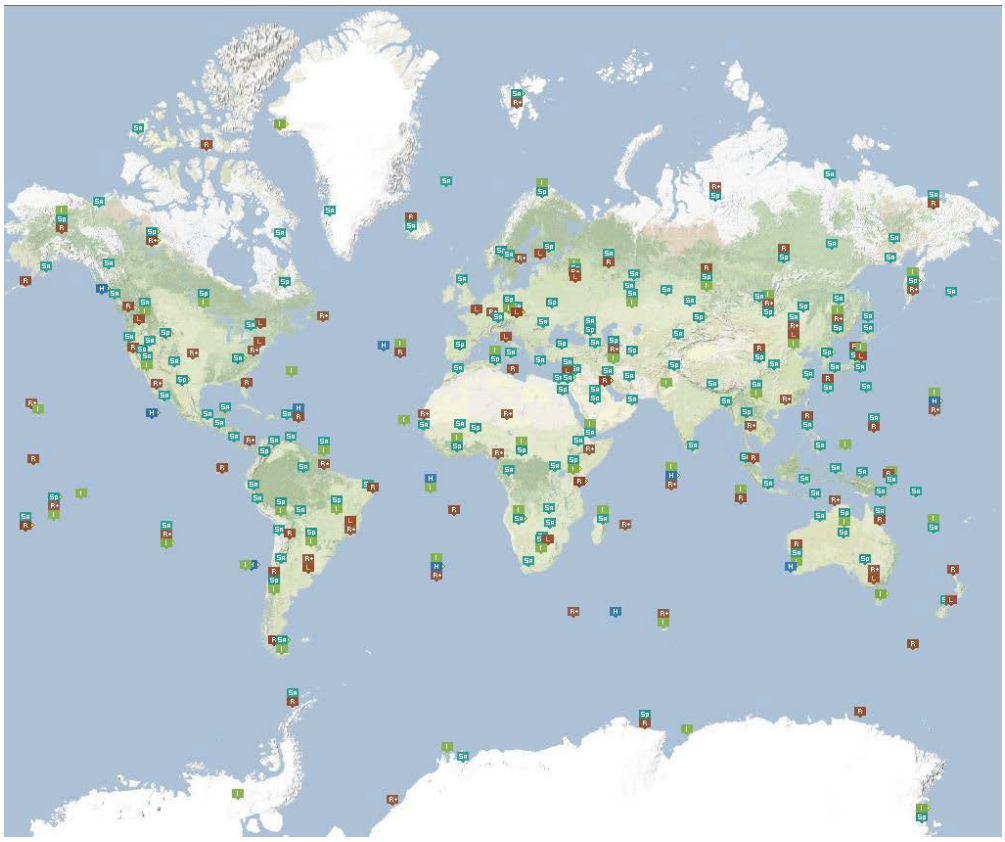

Figure 6: Confirmed IMS stations across the globe [43]

Figure 7: Radionuclide Stations in the IMS [32]

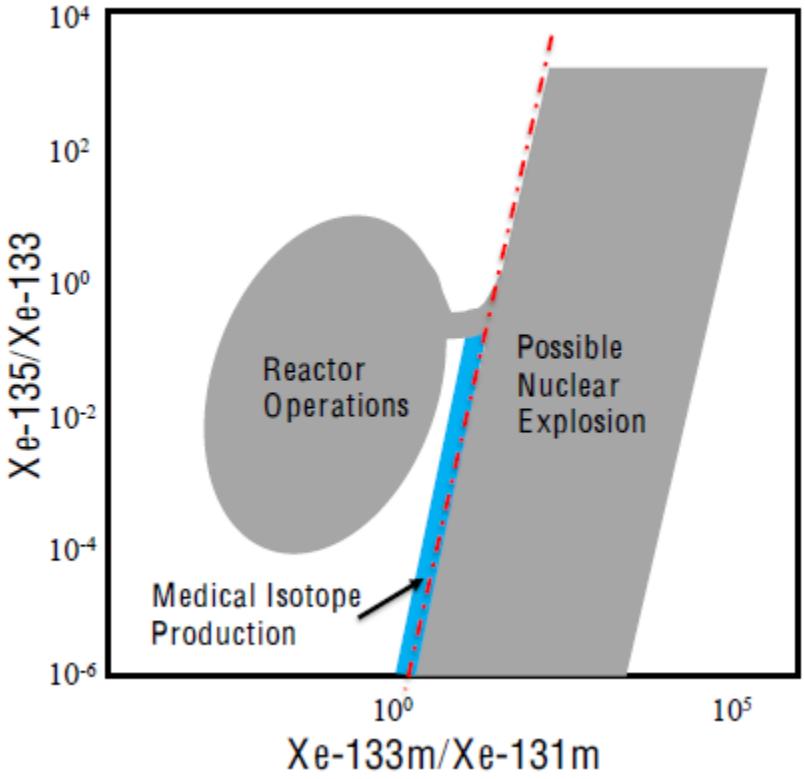

Figure 8: Radioxenon Ratio Comparison [44]

3.2. International Atomic Energy Agency

The International Atomic Energy Agency (IAEA) is the organization that oversees international cooperation pertaining to nuclear operations. As a result, the IAEA relies very heavily on on-site inspections to verify treaty compliance and ensure diversion activities are not being conducted by the host country. During an on-site investigation, inspectors are responsible for the following duties [45]:

- Identifying, Measuring, and Recording site characteristics;
- Obtaining Samples for Destructive Analyses;
- Environmental Sampling;
- Collecting, Inventorying, and Containing Samples;
- Understanding Material Flow and Inventory Balance for the site

The international nuclear proliferation policy was established by the IAEA with Information Circular (INFCIRC)/153 entitled “The Structure and Content of Agreements Between The Agency and States Required in Connection with the Treaty on Non-Proliferation of Nuclear Weapons.” In 1997, the agreement between states and the Agency was expanded in INFCIRC/540, also known as the Additional Protocol. The Additional Protocol is incorporated the direct requirements for the implementation of safeguards through accordance with Article III.1 of the Treaty on the Non-Proliferation of Nuclear Weapons (INFCIRC/140), which requires the state to accept safeguards on all source or special fissionable material with respect to all peaceful nuclear activities within its site boundaries and provides assurance and verification that material is not diverted to nuclear weapons or other nuclear explosive devices. While ensuring the security of nuclear material, the IAEA is conscious that unacceptable aggressive oversight could hinder the state both economically and technologically in an attempt to implement safeguards through non-obtrusive methods when feasible. INFCIRC/153 and INFCIRC/540 also provide what privileges and immunities are eligible to inspectors during an on-site investigation [46].

The IAEA receives its authority as an arm of the United Nations (UN) and applies its power based upon treaties and INFCIRCs. The content of INFCIRCs is determined by the purpose of each document, and can range from Nuclear Material Import and Export (INFCIRC/207- Notification to the Agency of Exports and Imports of Nuclear Material) to Safeguards (INFCIRC/808- Agreement Between the Principality of Andorra and the International Atomic Energy Agency for the Application of Safeguards in Connection with the Treaty on the Non-Proliferation of Nuclear Weapons). INFCIRCs can also be non-nuclear related or country specific [47].

Of the INFCIRCs available, the most well-known is the NPT (INFCIRC/140). The treaty, adopted in 1970 with 190 states subscribing, covers 3 main aspects: disarmament, non-proliferation, and peaceful uses of nuclear energy and technology. The core statement of the NPT is: “Countries with nuclear weapons will move towards disarmament; countries without nuclear weapons will not acquire them; and all countries can access peaceful nuclear energy and technology”. In support of this treaty (as well as the Additional Protocol), safeguards techniques

have been developed to ensure that nuclear technology will be encouraged to be used with peaceful intentions and that nuclear weapons research programs cannot be repurposed from research programs dedicated to peaceful means. Figure 9 elaborates on this verification and inspection process as dictated by the IAEA-TECDOC-1526 [47].

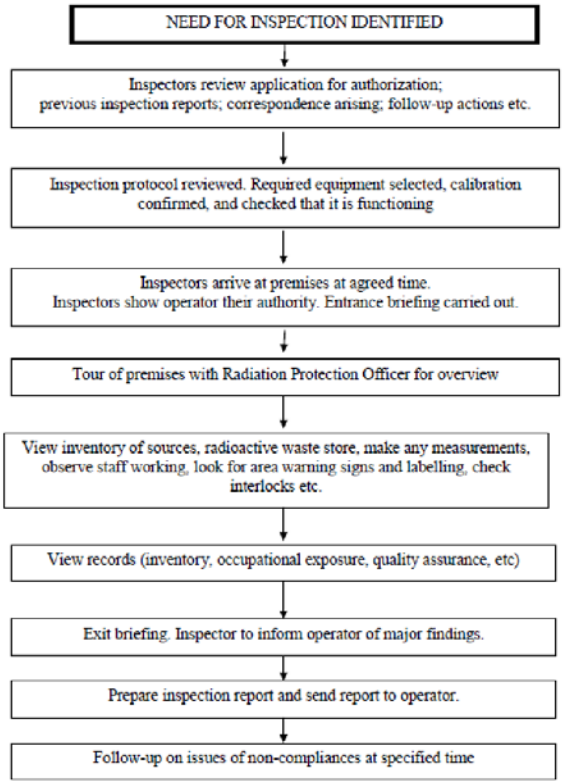

Figure 9: Flowchart for inspection process [48]

When an onsite inspection is conducted, several different inspection techniques are utilized. They are [49]:

- **Swipe Sampling** – This entails the collection of environmental residue from the vicinity of a known or suspected nuclear facility to sample for isotopics that would indicate separation operations being conducted. Environmental swipes can be taken to identify residual materials from a processing plant.

- **Multi-Channel Analyzers (MCAs) –** These are standard portable tools for IAEA inspectors to register the energy emitted by a radioactive source, and is designed to show radioactive hot spots and potentially identify the source and its location.

- **Alloy Detectors –** The alloy expert (ALEX) can be used to identify exotic steels and unusual elements based on their activity often used in metal scrapyards. Rapid, on-site identification of metals is a critical tool for inspectors. For example, uranium hexafluoride (UF_6) is highly-corrosive and its enrichment requires special materials. ALEX allows the IAEA to quickly determine whether the special metals are being stored on the site.

- **Environmental Monitoring Instruments –** Water and air monitoring are effective at determining whether or not a weapons research program exists. The water and air samples are examined for specific isotopes indicative of a weapons program.

- **Digital Video Surveillance Systems –** Tamper-proof video systems are used to monitor the activities in a facility. Inspectors review footage either on-site or remotely to determine if any actions made by the site personnel are fulfilling objectives other than those declared. For example, change in piping locations within a uranium enrichment cascade could indicate enrichment beyond declared levels.

- **Satellite Imagery –** Satellite imagery can provide inspectors with remote confirmation of construction projects, elevated or lack of personnel activity, or visual verification of mysterious objects. Similar to digital video surveillance systems, this can be used to see changes in site equipment that would indicate separation operations

Furthermore, the swipe samples take in on site investigations can be then sent back to the lab for post processing analysis. The post processing swipe samples can be utilized in several ways to assist in the detection of treaty violations. These capabilities include [50]:

- **High-Resolution Gamma Spectrometry –** A NDA screening tool to analyze and can be performed without removing samples from containers, reducing the chances of contamination.

- **Radioisotope X-Ray Fluorescence (XRF) –** NDA technique used specifically for uranium. Information from the XRF is used to determine future handling techniques of the sample, which limits the detailed analysis methods that can be applied later.

- **Scanning Electron Microscopy with Electron-Excited X-Ray Fluorescence Spectrometry (SEM/XRF)** – NDA Measurement technique for micrometer-sized particles. In particular, uranium/plutonium and plutonium/americium ratios are of interest in samples taken for material reprocessing sampling.

- **Thermal Ionization Mass Spectrometry –** A Destructive Assay (DA) ion-counting detector that can measure sub-nanogram uranium or plutonium masses. This process is used in conjunction with the SEM/XRF to obtain overall material composition.

- **Secondary Ion Mass Spectrometry –** This equipment is used to determine an isotopic concentration of U-235 to U-238 atoms from particles on the order of microns in length. This can be used in determining enrichment levels within a facility.

3.3. United States Department of Energy

Recently, President Obama reaffirmed the 2015 National Security Strategy by saying “No threat poses as grave a danger to our security and well-being as the potential use of nuclear weapons and materials by irresponsible states or terrorists [51]”. This statement reiterates that the utmost importance needs to be placed on ensuring that nuclear material is not obtained by individuals with criminal intent, and can be accomplished through proper emphasis on nuclear non-proliferation. In March of 2015, a report to congress was published entitled “Prevent, Counter, and Respond- A Strategic Plan to Reduce Global Nuclear Threats (FY 2016-FY 2020)”.

This report to Congress was submitted by the National Nuclear Security Administration (NNSA) of the Department of Energy (DOE) and is the first strategic plan of its kind on behalf of the National Nuclear Security Administration. The report covers three main topical areas, as outlined by the title [52].

- **Prevent –** "Non-state actors and additional countries from developing nuclear weapons or acquiring weapons-usable nuclear materials, equipment, technology, and expertise; and prevent non-state actors from acquiring radiological materials for a radiological threat device."
- **Counter –** "The efforts of both proliferant states and non-state actors to acquire, develop, disseminate, transport, or deliver the materials, expertise, or components necessary for a nuclear or radiological threat device or the devices themselves."
- **Respond –** "To nuclear or radiological terrorist acts, or accidental/unintentional incidents, by searching for and rendering safe, threat devices, components, and/or radiological and nuclear materials."

The report elaborates on each of these sections (Prevent, Counter, and Respond) as they regard to non-proliferation, material management, arms control, counter-terrorism, etc. and how NNSA will make decisions to adapt the prevent-counter-respond mission space to align with future program aspirations [52].

3.4. National Nuclear Security Administration

The NNSA strategic plan of May 2011 identifies five key goals in the coming years as the NNSA implements the responsibilities under the President's comprehensive nuclear security agenda:

- Reduce Nuclear Dangers;
- Manage the nuclear weapons stockpile and advance naval nuclear propulsion;
- Modernize the NNSA infrastructure;
- Strengthen the science, technology, and engineering base; and,
- Drive an integrated an effective Enterprise.

Reducing the national security threats due to nuclear proliferation is directly related to what has been discussed previously and is accurately described by the President stating, “There is no greater threat to the American people than weapons of mass destruction, particularly the danger posed by the pursuit of nuclear weapons by violent extremist and their proliferation to additional states [53].” Specifically within the DOE/NNSA, the NA-20 – Defense Nuclear Nonproliferation deals specifically with nonproliferation. This division is split into 6 different sub divisions [54]:

- NA-21 Global Threat Reduction
- NA-22 Nonproliferation Research & Development
- NA-23 Nuclear Risk Reduction
- NA-24 Nonproliferation & Informational Security
- NA-25 Material Protection and Cooperation
- NA-26 Fissile Materials Disposition

These offices as a part of NA-20 operation in conjunction with Department of Energy laboratories to develop technologies in advancing the U.S. Capabilities to detect and deter nonproliferation as well as serve as technology to verify treaties in conjunction with the IAEA. The office of Defense Nuclear Nonproliferation assists the DOE and NNSA to detect nuclear and radiological proliferation worldwide, while still collaborating with international states to ensure safe and peaceful uses of nuclear power. The core competencies of NA-20 are the following [52]:

1. Remove, eliminate, and minimize the use of proliferation-sensitive materials.
2. Safeguards and secure materials, technologies, and facilities.
3. Detect and prevent the illicit trafficking of nuclear/radiological materials, technology, information, and expertise.
4. Provide R&D technology solutions for treaty monitoring, minimizing the use of proliferation-sensitive materials, and the application of safeguards and security
5. Provide unique technical/policy solutions and develop programs/strategies to reduce nuclear/radiological dangers.

An underlying theme to all of these reports is the deterrence and detection of proliferation. The energy crisis posed to future generations will increase the demand of peaceful uses of nuclear power and the only way to ensure that these uses are kept peaceful is through assurance that proliferation is not occurring. All of the agencies mentioned previously will have to work hand in hand on order to assure proper collaboration on the topic of proliferation, not only to maintain currently technology, but to develop new technology that will function more effectively and decrease any chance for errors in the detection of proliferation.

4. Case studies

Given the current medical isotope usage, the medical field will only increase the usage of radioisotope therapy. Furthermore, current trends of energy demands and economics of nuclear energy indicate that the abundance of nuclear technology used for civilian power will increase as well. In conjunction with the desire to safeguard material appropriately, knowing where medical isotope facilities are located as well as the amount of material used is and will be a growing concern, especially when several facilities require high enriched uranium to achieve the desired flux to produce isotopes.

After the attack on the United States on September 11, 2001, the United Nations (UN) became very concerned with the potential of terrorists using weapons of mass destruction (WMD) in future attacks in the US or other UN member states. In order to address this, the UN established Security Resolution 1540, which established twelve ways to facilitate an effective response to the area of nonproliferation. In summary, these facilitating modes establish how member states approach deterring, detecting, and preventing non-state members to manufacture, acquire, possess, develop, transport, transfer, or use nuclear, chemical or biological weapons and their means of delivery. These measures were soon adopted under chapter VII of the UN Charter in 2004. [55]

From an international standpoint, the UN and IAEA are responsible for the actions and their implementation to deter proliferation of WMD. From a domestic standpoint, the United States applies several agencies to deter, detect, and prevent domestic acts of terrorism. Some of

these agencies are: the Department of Energy, the National Nuclear Security Administration, the Department of Homeland Security, and the Department of State.

4.1. History of Safeguards

Even though medical isotope production and nuclear weapons predate the ending of World War II, the concept of nuclear safeguards can be traced back to the early years of the Cold War. During this period, both the US and Soviet Union were drastically increasing their respective weapons development programs. As member states of the United Nations become increasingly concerned with the accelerated developments, the UN constructed the first treaty overseeing nuclear weapons development by differentiating between weapons, and non-weapons states in an attempt to limit the number of countries pursuing nuclear weapons in the future. Two years after this, the NPT was generated in conjunction with the associated scope of safeguards to be implemented by the IAEA as guided by the UN [45].

Furthermore, in 1971, the UN founded a committee under Chairman Claude Zangger (the Zangger Committee) to establish a trigger list of source or special fissionable material and the equipment or materials especially designed to prepare for the processing use, or production of special fissionable materials. The first trigger list that was produced as a result of this committee was INFCIRC/209 and the latest revision of INFCIRC/209 took place June 2014 with Revision 3 [55] [56].

4.2. Iran

The history of Iran’s use of nuclear research reactors dates back to the Atoms for Peace program when the Tehran Research Reactor (TRR) was provided to the Shah of Iran in 1967. The original research reactor utilized 93% enriched HEU, with the first shipment supplied in 1967 [57]. Twenty years later, in 1967, Argentina concluded a deal to convert the reactor core from 93% to 20% enriched fuel, which is considered low enriched uranium (LEU), based on an agreement from 1985. The of sale of 115.8 kg of 20% reactor fuel was approved by the IAEA, in

which the Argentina's Investigaciones Aplicadas (INVAP) was selected to supply the reactor fuel.

The timeline for the beginning of Iran's nuclear research program represents multiple achievements of nuclear safeguards. The main achievement is the use of nuclear power for peaceful purposes. Several treaties have been put in place to ensure that nuclear power is being used for peaceful purposes with continual monitoring of these facilities to ensure that these reactors are not being used to produce other materials for a weapons research and development program (as specified in the NPT). The establishment of the TRR in 1967 showed that this goal was achievable. The next safeguards achievement was the conversion of this reactor from 93% to 20% enriched uranium. As technologies advance and the need for HEU becomes less necessary, conversion of research reactors to LEU fuel means that the probability of producing material for a weapons program will be decreased and required safeguards and security for this site will be less critical. Since uranium required for weapons development requires very high enrichment (past 90%), decreasing the fuel enrichment in a reactor and adding other material, such as molybdenum or zirconium alloy, will make the material unusable for a weapon and prevent the reprocessing of the material due to the additives [17].

4.3. Israel

Israel's desire to establish a research reactor was established in 1953 with the co-operation agreements that concluded between Israeli Atomic Energy Commission and France's Commissariat à l'énergie atomique. This agreement enabled the French Government to supply Israel with a 25 MW research reactor [58]. Although this agreement was not implemented immediately, the United States supplied a pool-type light-water reactor that began operating in June of 1960. The Nahal-Soreq research reactor (IRR-1) uses 90% enriched uranium and original operated at a 1 MW capacity, with an expansion to 5 MW by 1969. Israel's nuclear research capability was soon augmented with the establishment of the Dimona reactor, which functions through the use of natural uranium and is heavy-water moderated [58]. The initial capacity of this reactor was 25 MW and was built with the help of French scientists and engineers. An initial supply of 20 to 25 tons or uranium was needed, but concerns arose because of the potential

production of plutonium within the reactor that could range from 8 to 10 kg of unseparated material, annually. If reprocessed, this could produce a significant quantity of plutonium.

Since the establishment of these reactors, several concerns have emerged from the Dimona reactor. At some points in its forty year history, potassium iodide tablets were distributed to nearby residents due to the age of the facility. The reactor was shut down in January of 2012 due to vulnerabilities of the site to attack.

Although these facilities do not demonstrate the enrichment reduction achievements motioned in the previous Iran chapter, this case study addresses a different mode of success – shutting down a reactor due to vulnerabilities. The acknowledgement that the facility had significant vulnerabilities to attack shows the commitment of different counties to utilize nuclear facilities responsibly and for the proper reasons.

5. Signature Isotopes

In order to sample for a medical isotope facility, a signature that is specific to a medical isotope facility needs to be determined. As mentioned in previous sections, radioxenon is a very good indicator of nuclear activity. These radionuclides are sampled for by the CTBTO when monitoring for nuclear detonation and are also well-suited radionuclides to sample for when detecting any sort of nuclear facility, specifically a medical isotope production facility. Due to the noble gas nature of xenon, it is very difficult to capture the isotopes of xenon before they are released into the environment.

5.1. Radioxenon

The two isotopes of radioxenon that are of interest are xenon-133 and xenon-135. Of the different isotopes of xenon, only 6 of the isotopes out of 40 known isotopes of xenon have a half-life greater than 1 hour: ^{122}Xe, ^{123}Xe, ^{125Xe}, ^{127}Xe, ^{133}Xe, and ^{135}Xe. Table 2 elaborates on the different isotopes of xenon and their associated properties.

Table 2: Nuclides of Interest for Xenon [33]

Isotopes	Natural Abundance (At %)	Half Life	U-235 Fission Yield	Pu-239 Fission Yield
Xe-124	0.1		blocked	blocked
Xe-125		17.1 hr	blocked	blocked
Xe-126	0.09		blocked	blocked
Xe-127		36.4 d	blocked	blocked
Xe-128	1.91		blocked	blocked
Xe-129	26.4		blocked	blocked
Xe-130	4.1		blocked	blocked
Xe-131	22.2		2.89%	3.86%
Xe-132	26.9		4.31%	5.41%
Xe-133		5.243 d	6.70%	7.02%
Xe-134	10.4		7.87%	7.68%
Xe-135		9.10 hr	6.54%	7.60%
Xe-136	8.9		6.32%	7.10%

The two most interesting and useful properties of radioxenon are listed in the final two columns of Table 2– the fission yield for both U-235 and Pu-239. The fission from U-235 and Pu-239 are the main contributors to fission within the reactor, and the characteristics provide an excellent representation of the reactor fuel, and consequently the facility, as a whole. The fission yield percentages for radioxenon, as shown in Table 2 seem low, but are actually very high fission product yields when considering the entire fission product distribution (Figure 11). Looking at the isotopes of Xe-124 through Xe-128, Table 2 indicates that the fission yields for these isotopes are “blocked”. This means that isotopes of tellurium and iodine block the fission production of these isotopes. Upon further investigation of Table 2, there are only two other

isotopes that remain as viable fission product yields that are radioactive. These two products are xenon-133 and xenon-135.

In order to determine the rate of xenon-133 and xenon-135 production as a function of the fission, the fission reaction rate must be determined. Once the fission reaction rate is determined, simply multiplying that value by the yield will result in the creation of xenon within the reactor. This can be done through the application of Equation 1, where σ_f is the fission cross section and ϕ is the neutron flux. Assuming the flux is similar to that of the HFIR reactor in Oak Ridge ($5*10^{15}$ $\frac{n}{cm^2 s}$) [36] and the cross sections for U-235 and Pu-239 are both about 10^3 barns (displayed in Figure 10), these reactions, combined with the fission product yields discussed previously, result in reaction rates represented in Table 3.

Equation 1: Fission Reaction Rate

$$RR_{fission} = \sigma_f * \phi$$

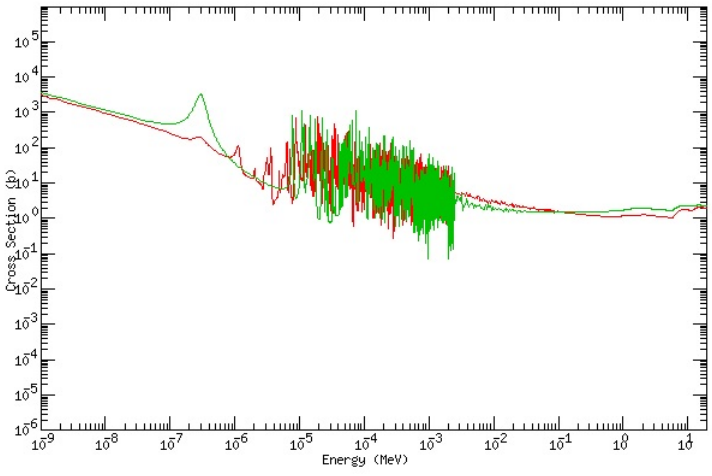

Figure 10: Fission Cross Sections for Pu-239 (green) and U-235 (red)

Table 3: Reaction Rate Calculation Results

	Xenon-133	Xenon-135
Uranim-235	2.68E-7 s^{-1}	2.616 E-7 s^{-1}
Plutonium-240	2.808E-7 s^{-1}	2.616E-7 s^{-1}

Another significant source of xenon is through the spontaneous fission of plutonium-240. Plutonium-240 is an isotope that naturally builds up in reactors through neutron absorption of plutonium-239. Typically, when considering plutonium for weapons purposes, a content of <8% ^{240}Pu is required due to the spontaneous fission rate, which can cause predetonation. However, for this study, spontaneous fission is viewed as a positive phenomenon because of the natural accumulation of radioxenon. The half-life of plutonim-240 is 1.1E11 years [33]. With this half-life, the decay constant, λ, can be derived through Equation 2. By applying the known half-life, the decay constant of plutonium-240 is 1.93E-19s^{-1}. In order to determine what the accumulation of each isotope of xenon is in relation to this decay constant, the spontaneous fission yield of that specific isotope is then multiplied by the decay constant. The spontaneous fission product yield for xenon-133 and xenon-135 from plutonium-240 is 7.02% and 7.6% respectively [44]. Thus, the accumulation of the isotopes xenon-133 and xenon-135 will be $\lambda_{Pu\text{-}40}$*yield which is 1.35E-20s^{-1} and 1.46E-20s^{-1} respectively. When comparing these reaction rates to that of the fission reaction within a reactor, they are negligible since they differ by a factor of 10^{13}. For material that has been removed from the reactor for a long period of time, induced fission reactions have dropped to almost zero and spontaneous fission occurs more frequently. However, as this scenario examines material that was recently irradiated within a reactor with up to $5*10^{15}\ \frac{n}{cm^2 s}$, this production mechanism of radioxenon will not be accounted for.

Equation 2: Decay Constant Definition

$$\lambda = \frac{ln(2)}{T_{\frac{1}{2}}}$$

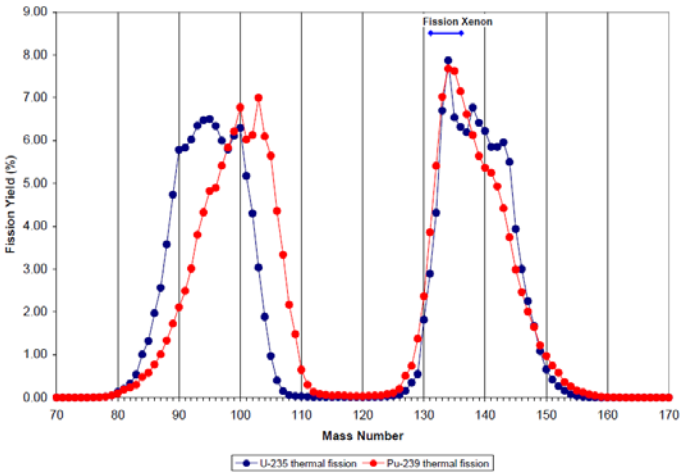

Figure 11: Fission Product Yield for U-234 and Pu-239[33][59]

5.2. Detection of Radioxenon

Two xenon isotopes have been identified as viable isotopes to sample for when investigating for a thermal fission event of U-235 or Pu-239, so the next technical parameter required is the detection limits of these two isotopes. In experiments conducted at Pacific Northwest National Labs, an objective was established to identify buried transuranic waste. This study investigated the capabilities of detecting this waste through the sampling of radioxenon, specifically xenon-133 and xenon-135. Samples were taken from the 200-West Area at PNNL containing a combined 16,400 $\frac{mBq}{m^3}$ of xenon-133 and 1,811$\frac{mBq}{m^3}$ as shown by Figure 12. The outcome of this study determined the detector limits for both xenon-133 and xenon-135, which are 0.58$\frac{mBq}{m^3}$ and 3 $\frac{mBq}{m^3}$, respectively [33]. These detection limits are the minimum activity per cubic meter that are required in order to positively detect a presence of xenon-133 and xenon-135 above background levels. Positive detection above this limit would indicate the presence of a nuclear fission facility or device being utilized in which some amount of radioxenon has escaped.

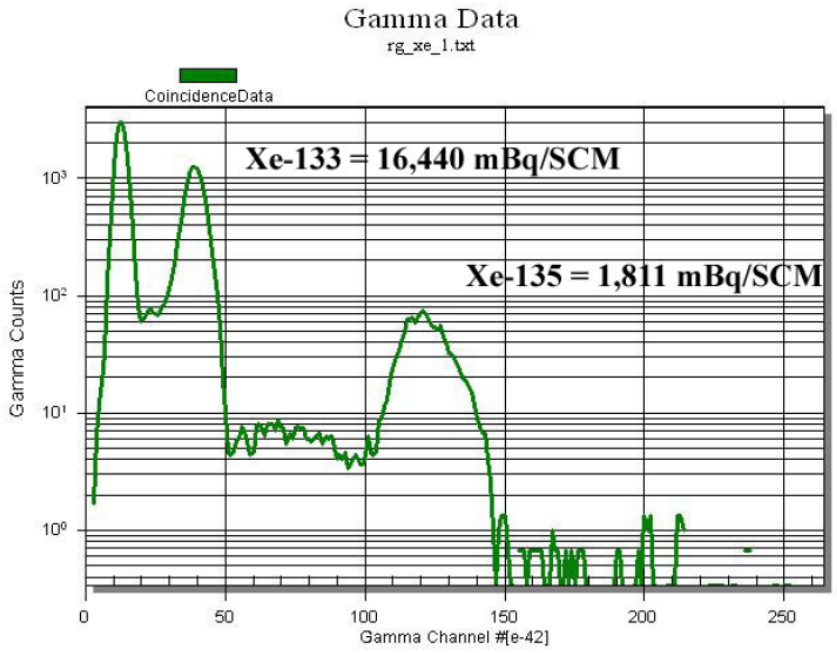

Figure 12: Gamma Spectrum taken at 200 Area West for the PNNL Study [33]

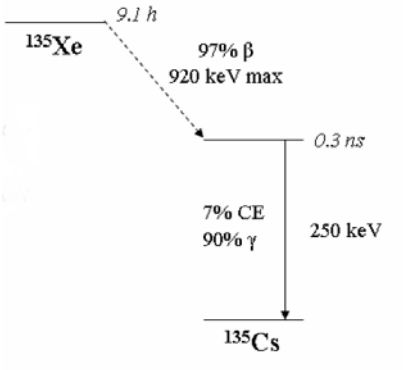

Figure 13: Decay Scheme of xenon-135 [44]

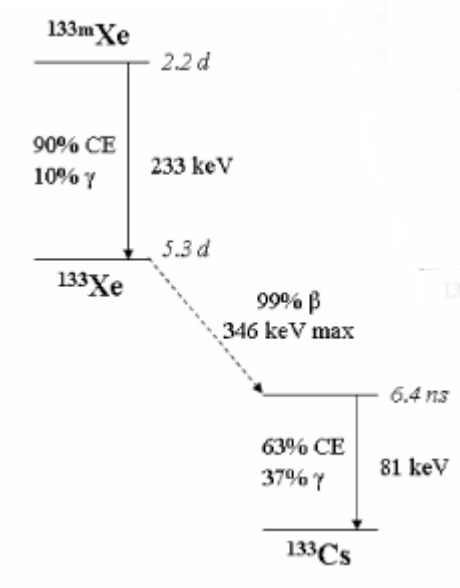

Figure 14: Decay Scheme of xenon-133[44]

The detection of xenon occurs through a coincidence counting of the beta and gamma particles emitted in the radioactive decay of the xenon isotopes. The concept of coincidence counting is common throughout the radiation detection research industry and can assist in the

detection of radionuclides that emit a low energy gamma ray, which is of interest to both the Xe-133 and Xe-135 detection. Xe-133 decays by emitting an 81 keV gamma in 37% of its decay events along with a 346 keV maximum energy beta particle. This gamma ray can be very difficult to detect as it is commonly drowned out by noise or characteristic X-rays from lead shielding. Xenon-135 is identified through the detection of the emitted 910 keV beta particle in coincidence with a 250 keV gamma which occurs 97% of the time [33]. One example of technology that utilizes this counting method is a phoswich detector [60]. A phoswich detector is a type of scintillation detector that implores two different scintillation materials using the same photomultiplier tube (PMT). Through the use of two different material types, two pulse decay times will occur. Though this difference of decay time the pulses can be distinguished from one another. When two pulses occur simultaneously, a joint beta-gamma interaction is represented. This then allows the gamma interaction pulse to be processed in the pulse height analyzer and then sent to the multi-channel analyzer for spectroscopy [60]. At the gamma energies for xenon-133 and xenon-135, large background levels occur due to electronic noise and the Compton continuum thus sampling for these gammas in coincidence with their beta max energy will reduce the background noise significantly. An example of recent technologies that implements beta-gamma coincidence counting is the Automated Radioxenon Sampler-Analyzer (ARSA). This technology is implemented for post sampling analysis and processes data from two the two different detector types to examine the concentrations different radioxenon isotopes.

Recent research has been conducted on how to better characterize the amount of xenon within a collected sample. In the same PNNL study mentioned previously [33], by running a xenon sample through a quadruple mass-spectrometer, detection capabilities are increased. By dropping the MDA to 0.15 $\frac{mBq}{m^3}$ and 0.3$\frac{mBq}{m^3}$ for ^{133}Xe and ^{135}Xe, respectively [33], the detection limits can be decreased by a factor of ten. Although these MDAs are very convenient, this will not be investigated further within this research since MDAs at such a low value require very unique instruments as well as an 8 hour collection time [33].

6. Research Presentation

The purpose of this research is to create a calculable model that would be useful in determining the probability of detecting a medical isotope production facility through environmental sampling for Tc-99m, I-131, etc., which directly pertains to the verification technology the IAEA utilizes in their efforts. A positive detection will indicate that the particulate is detected above minimum detectable activities or quantities. A negative or null sampling result could indicate the levels of particulate are below detectable levels or that there is not particulate to detect.

6.1. Research Objective

This research is accomplished through a series of repeated random sampling (Monte Carlo-based sampling) simulations concerning two specific environmental conditions, wind speed and direction. Once the conditions are determined, a plume model can be created using the Gaussian plume equation. The developed model requires a source term that represents the concentration of an isotope emitted by medical isotope facility. As a result, the value source term will be the primary variable of interest. After the plume is created, a geographic location will be selected using Monte Carlo sampling from a predetermined probability distribution function (PDF) representative of the population. Finally, the atmospheric distribution of the source will be represented by a Gaussian plume distribution of the quantities or activities. If the activity or quantity on a given mesh point is greater than or equal to the minimum detectible amount, the point will indicate a ‘positive detection’. Conversely, if the activity or quantity is less than the limit, a ‘negative detection’ will result. The following subsections will elaborate on each part of the simulation and will go into detail on how each aspect of the simulation is accomplished, as well as the supporting items that support that the method functions as desired.

6.2. Environmental Condition Sampling

In order to sample for environmental conditions using Monte Carlo methods, data needs to be accumulated in order to form a PDF that is representative of this data. An environment of interest is one that is very dry and arid to promote the transportation of particulates. Considering these conditions, the Southwest region is the best environment that represents this within the

United States. More specifically, a location within that region must have the availability to obtain data pertaining to the climate conditions. Given these constraints, a location that best fits the criteria is Albuquerque, New Mexico. Albuquerque provides a very dry and arid environment that resembles the circumstances desired when considering an isotope separation location. Additionally, there is plenty of information pertaining to the climate within the area for Sandia National Laboratories and Kirtland Air force Base [51].

Information regarding wind speed and direction can be obtained from the National Oceanic and Atmospheric Administration (NOAA) National Climate Data Center. By compiling climate information dating back to January of 2009, a histogram can be created that represents both the wind speed in meters per second as well as wind direction in degrees. The histogram can be viewed as a discrete PDF. However, due to the lack of continuity, simple inverse transform sampling cannot be applied because there is no function that exactly fits the data. Therefore, the concept of rejection sampling must be utilized.

Rejection sampling utilizes two separate functions. The first function is the PDF that contains the data in which one is sampling from. The second function retains a value that, for all values of x, is greater than the PDF, M(x). These two functions are expressed in Figure 15. Furthermore, Figure 16 and Figure 17 show the data used and the associated containing functions.

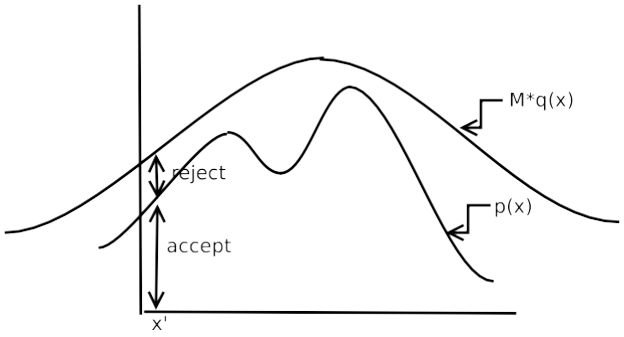

Figure 15: Containing Function and PDF [62]

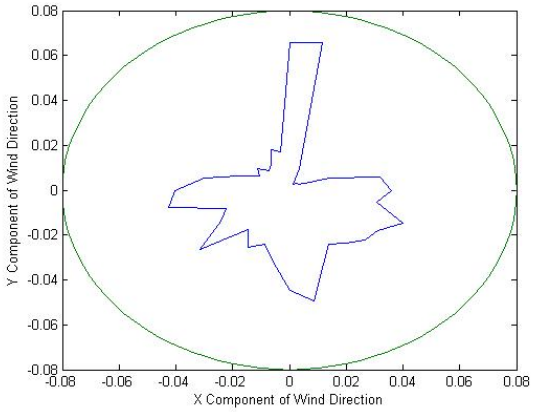

Figure 16: Wind Direction PDF and Containing Function

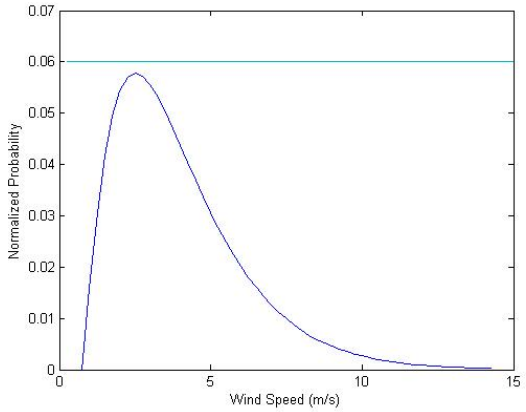

Figure 17: Wind Speed PDF and Containing Function

Given the two functions, two random numbers will be generated. The first random number, R1, represents a span between the minimum x value and the maximum x value in which both the containing function and the PDF will be sampled from. The second random number, R2, represents a number between zero and the containing function evaluated at R1. The algorithm for sample rejection is as follows [62]:

1. Generate R1 between 0 and the maximum x value
2. Evaluate M at (R1)
3. Generate R2 between 0 and M at(R1)
4. If R2< (PDF at (R1))
    a. Use PDF at (R1) as sample
5. Else if R2>PDF at (R1)
    a. Reject sample
6. End if
7. Repeat as desired

As the number of samples gets larger, the normalized sample histogram should trend toward the PDF. This trend is shown in both Figure 18 and Figure 19, where different sample numbers were taken from this algorithm.

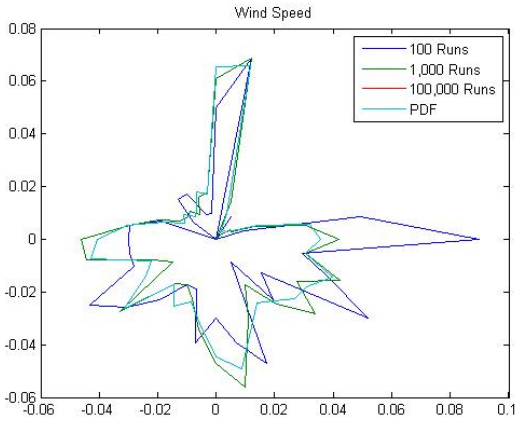

Figure 18: Wind Directions PDF and Histograms

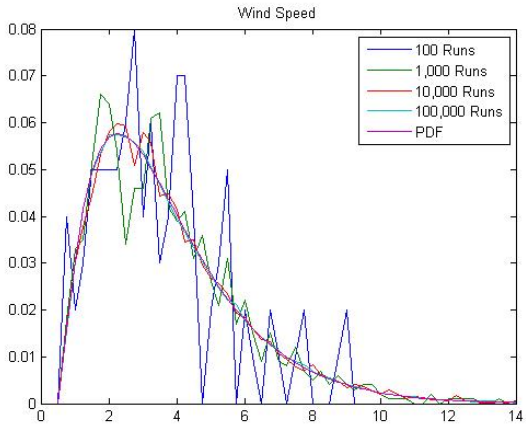

Figure 19: Wind Speed PDF and Histograms

The trend shown above in both figures supports the statement that as the sample pool becomes significantly large, the algorithm reproduces the PDF.

6.3. Location Sampling

Similar to the environmental sampling, location sampling will utilize Monte Carlo methods to determine the location of the source plume. The distribution assumes a single node population where the center of the city has the largest density and decreases in an inverse quadratic function [63]. Additionally, a mesh established with a grid spacing of 0.1 kilometers is established due to the limitations of sampling points. Finally, a quasi-random location is determined for both the longitude and latitude of the source using the same algorithm as the environmental monitoring and rejection sampling. This mesh will also represent the sampling locations for the plume. Figure 20 and Figure 21 represent the longitude and latitude sampling and the trend towards the PDF as the sample pool becomes large enough. Therefore this representation supports the rejection sampling method. Lastly, Figure 22 shows the exact Population Density Function used for this simulation.

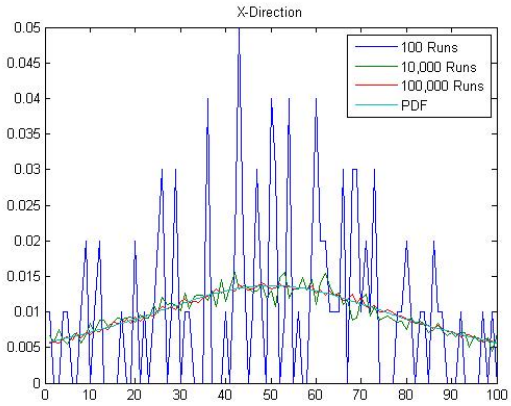

Figure 20: X Direction Source Location PDF and Histograms

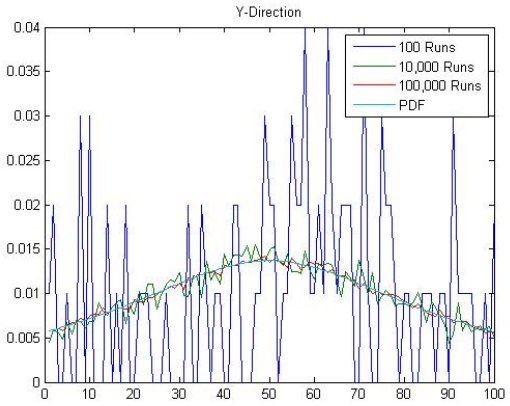

Figure 21: Y Direction Source Location PDF and Histograms

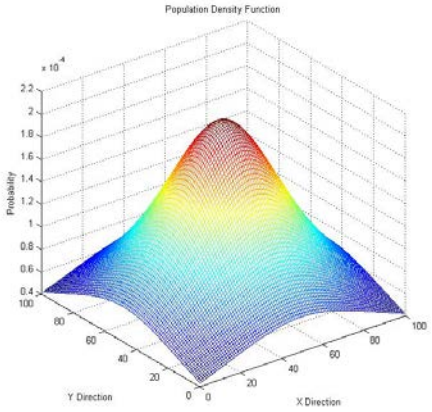

Figure 22: Population Density Function

6.4. Plume modeling

As the environmental conditions and location have been determined, all the necessary information has been obtained to perform a plume calculation. A Gaussian plume equation in its most generic form will be used in order to create multiple plumes with accurate distributions while maintaining an efficient computing time (Equation 3). Figure 23 shows all the variables and their relation to the plume. [64]

Equation 3: Generic Gaussian Plume Equation

$$\mathrm{X}(x,y,x,h) = \frac{Q}{2\pi U\sigma_y\sigma_z}\exp\left[-\frac{y^2}{2\sigma_y^2}\right] * \left\{\exp\left[-\frac{(z-h)^2}{2\sigma_z^2}\right] + \exp\left[-\frac{(z+h)^2}{2\sigma_z^2}\right]\right\}$$

Where

Q is the source emission rate (Ci/s or g/s),

U is the average wind speed at stack height (m/s),

σ_y, σ_z are the standard deviations of the concentration distributions in the crosswind and vertical directions (m),

h is the effective stack height (m),

x is the distance downwind from the stack (m),

y is the crosswind distance from the plume centerline, and

z is the vertical distance from ground level.

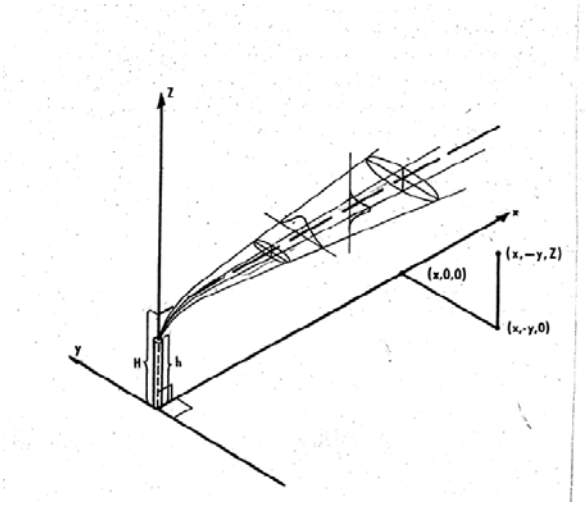

Figure 23: Coordinate system for Gaussian Plume Equation. [64]

When using this equation, several assumptions are made pertaining to the simulation. The assumptions are as follows [64]:

1. The emission rate is constant
2. Dispersion (diffusion) is negligible in the downwind (x) direction
3. Horizontal meteorological conditions are homogenous over the space being modeled. These conditions include:

   a. Average Wind Speed
   b. Wind Direction
   c. Temperature
   d. Atmospheric stability class
   e. Mixing height
4. No wind sheer in horizontal or vertical direction
5. Plume is infinite with no plume history (each simulation is independent)
6. Pollutants are non-reactive gases or aerosols that remain suspended in air following the turbulent
7. The plume is reflected at the surface with no deposition or reaction with the surface
8. The dispersion in the crosswind (y direction) and vertical (z direction take the form of Gaussian distributions about the plume centerline.

In this equation, several parameters have been determined through the Monte Carlo Sampling methods. These variables include the average wind speed, U (m/s), and the plume location origin (x, y, z). However, there are still parameters that have yet to be defined such as the standard deviation of the cross sections for both the crosswind (y) and vertical (z) directions. These variables are a function of the mean wind speed and the distance downwind from the source. Once the variables are appointed, coefficients are assigned to a power law equation for both cross section distributions, which are described in Equation 4 and Equation 5. The equations, however, are dependent on the stability class that the environmental conditions fall into. The conditions and their related stability classes are listed in Table 4.

Equation 4

$$\sigma_y = cx^d$$

Equation 5

$$\sigma_z = ax^b$$

where x is the downwind distance and the a, b, c and d coefficients are decided using Table 4 and Table 5

Table 4: Stability Class Description [64]

Stability Description	Stability Class
Extremely Unstable	A
Moderately Unstable	B
Slightly Unstable	C
Neutral Conditions	D
Slightly Stable	E
Moderately Stable	F

Table 5: Power Law Exponents and Coefficients for Vertical Distributions [64]

Power Law Exponents and Coefficients for σ_z						
Atmospheric Stability Class	Downwind Distance, meters 100< x<=500		Downwind Distance, meters 500< x<=5000		Downwind Distance, meters 5000< x	
	a	b	a	b	a	b
A = 1	0.0383	1.281	0.0002539	2.089	0.00025	2.089
B = 2	0.1393	0.9467	0.04936	1.114	0.04936	1.114
C = 3	0.112	0.91	0.1014	0.926	0.1154	0.9109
DD = 4	0.0856	0.865	0.2591	0.6869	0.7368	0.5642
DN = 5	0.0818	0.8155	0.2527	0.6341	1.297	0.4421
E = 6	0.1094	0.7657	0.2452	0.6358	0.9204	0.4805
F = 7	0.05645	0.805	0.193	0.6072	1.505	0.6332

Table 6: Power Law Exponents and Coefficients for Vertical Distributions [64]

Power Law Exponents and Coefficients for σ_y				
Atmospheric Stability Class	Downwind Distance, meters x<10,000		Downwind Distance, meters x>=10,000	
	c	d	c	d
A = 1	0.495	0.873	0.606	0.851
B = 2	0.31	0.897	0.523	0.84
C = 3	0.197	0.908	0.285	0.867
DD = 4	0.122	0.916	0.193	0.865
DN = 5	0.122	0.916	0.193	0.865
E = 6	0.0934	0.912	0.141	0.868
F = 7	0.0625	0.911	0.08	0.884

The next variable of interest is the stack height, which will remain constant through the entire simulation and will not be a function of any parameters. Several studies have been conducted on detecting chemical processing facilities and the stack heights considered range from 15-45 meters. The larger the stack height, the further downwind the plume deposit activity or concentrations will peak. As a result, an investigation for stack height ranging from 0 meters (ground level) to 45 meters will be conducted prior to the main simulation as to determine the most vulnerable stack height. Having a larger stack height has its benefits and drawbacks. The plume deposit will occur further away from the facility; however, due to facility specifications, a large stack height could not an option. Considering these different scenarios will provide a well-rounded analysis and different insight into facility detection [65].

The next and final variable to consider is the source of the plume. The Gaussian plume model is capable of dealing with 5 different types of plume sources [64]:

A. Point Source – a single emission point with a continuous emission rate (i.e. smoke stack).

B. Volume Source – uses a virtual point set where user sets height, and virtual horizontal and vertical dimensions (i.e. conveyer belt).
C. Area Source – emission from an area that is rectangular in shape where use sets height and size (i.e. dump)
D. Open pit – represents emissions from an open pit below grade (i.e. a mine).
E. Flare – non continuous emission where the heat goes to combustion and buoyancy of plume.

Given the possible scenarios, the best fitting representation of the desired situation is type A, the point source, which represents a stack coming out of the isotope production facility. The next piece of information needed pertaining to the source is the emission rate of the facility. The term, *Q*, represents the release in units of Curies (Ci) per second and thus the amount released into the environment needs to be represented accordingly. The different emissions will be dependent upon the material production rate of the medical isotope facility and will be the main variable of investigation for this research. Release rates on the order of millicuries (mCi) to be utilized will range from 12 mCi per second and to 63 mCi per second.

Since all variables are established, the Gaussian plume can be created through the use of a special mesh on the X and Y plane. The mesh has a spacing of 0.1 km (100m). Through trial and error, this spacing was the best fit that would yield an effective sampling rate while still allowing a large enough sampling pool. Figure 24 shows an example of a Gaussian Plume created within MATALB. This is the same plume that will be used in the future simulation.

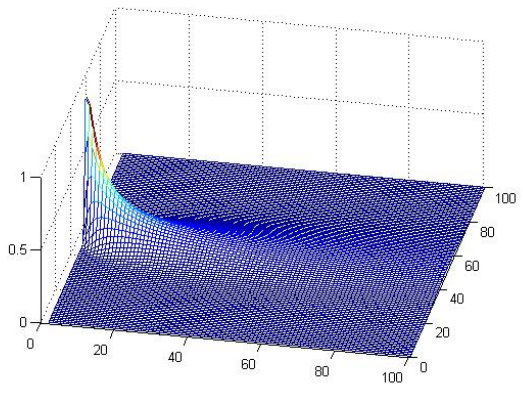

Figure 24: Normalized Gaussian Plume used in Simulation

6.5. Simulation

With all variables and PDF's defined, it is possible for the simulation to be conducted. First, the random variables will be sampled (mean wind speed, wind direction, and source location) to enable the calculation of the vertical and horizontal wind cross section distributions. The characteristic plume can be created by applying the source strength as determined by the simulation type. This plume will be applied to the special mesh (100 meter spacing). Then, a positive or negative detection will be determined by comparing the concentration amounts at each node with the detection limits. The detection limits, however not 100% certain, will yield an accurate detection within the 99.87 percentile (3 standard deviations). If the plume is positively detected, a '1' will be added to the total detection sum. If the plume is not detected, a '0' will be added to the total detection sum. This process will be repeated through a predetermined number of plume creations and when complete, will have a given number of positive detections. By dividing this number with the total times the simulation was conducted, a total probability of detection can be established for the simulation type. Further investigation beyond the polar question of detection will be conducted by examining the probability of detection as a function of the distance from the source.

7. Results

As stated previously, a medical isotope facility producing Tc-99m will be considered. The circumstances considered will have different release rates of radioxenon within the range of Curies per year. Within these two activities, five different processing rates will be considered. Table 7shows the different reprocessing rates for each activity.

Table 7: Nuclear Material Processing Rates

Case Number	Source Term (Ci/year)
1	2.0

2	1.6
3	1.2
4	0.8
5	0.4

For each scenario, 1,000 Plumes were created all independent of one another. The only similarity between the plumes is the source term, which is a function of the scenario being considered. Furthermore, each scenario was run 10 times to ensure that all detection probabilities are reported properly with the associated standard deviation. The detection probability as a function of the distance was reported as averaged over the 10 runs with associated error bars. Furthermore, an example plume centerline concentration was reported because the centerline is where the highest concentrations exist. The plume centerline equation, shown in Equation 6, was created through simplification of the Gaussian plume equation (Equation 3).The plume centerline is only a function of the x variable and expressed as:

Equation 6: Plume Centerline Concentration

$$\mathrm{X_{CL}}(x,y,x,h) = \frac{Q}{2\pi U\sigma_y\sigma_z} * \left\{ \exp\left[-\frac{(z-h)^2}{2\sigma_z^2} \right] + \exp\left[-\frac{(z+h)^2}{2\sigma_z^2} \right] \right\}$$

Further simplifications were obtained through the ground level (z=0) assumption. This simplification resulted in Equation 7:

Equation 7: Ground Level Assumption

$$\mathrm{X_{CL,G}}(x,y,x,h) = \frac{Q}{2\pi U\sigma_y\sigma_z} * 2\left\{ \exp\left[-\frac{(h)^2}{2\sigma_z^2} \right] \right\}$$

Lastly, it was possible to determine at what x variable along the plume centerline the concentration was highest through taking the derivative of Equation 5, setting it equal to 0, then solving for the associated x value. In order to do this, replacing the values of $\sigma_y = cx^d \; and \; \sigma_z = ax^b$ ensured no unknown variable. After doing this, Equation 8 was calculated as:

Equation 8: Location of Maximum Concentration

$$x_{max,CL} = \frac{\ln\left(\frac{bh^2}{a^2(d+b)}\right)}{\ln(b-d)}$$

This derivation can be found in Appendix A.

The next sections present the data obtained from the simulations run pertaining to the material processing rates. Each simulation will have 10 runs each with 1,000 simulated plumes per run.

7.1. Stack Height Variation

As previously mentioned, the stack height for the facility (either reprocessing or uranium enrichment) is a necessity to provide airflow in the facility. This stack will be treated as the source location for the material release and thus is a very variable within the simulation. The stack height of interest range from 0 meters tall (ground level) all the way up to 50 meters tall. Figure 25 provides a graphical representation of how the plume centerline concentration is impacted by the stack height. Figure 25 shows two different trends. As the stack height is increased, the peak plume value is decreased, a result supported by Equation 8 since the peak concentration point is proportional to the stack height. The next trend shown by the figure is a shifting of the peak downwind, which is dependent on the wind speed correction factor in Table 8. When applying the wind speed correction factor to Equation 8 as the stack height increases, the wind speed will increase proportionally to the ratio of the stack height to the wind speed sample height raised to a form factor established by the atmospheric stability class and wind speed. Logically, larger stack height values will result in a farther distance the release travels before reaching ground deposition.

Equation 9: Wind Speed Adjustment for Stack Height

$$U_z = U_0\left(\frac{Z}{Z_0}\right)^p$$

Table 8: Wind Profile Exponent

Stability Class	Rural exponent	Urban exponent
A	0.07	0.15
B	0.07	0.15
C	0.10	0.20
D	0.15	0.30
E	0.35	0.30
F	0.35	0.30

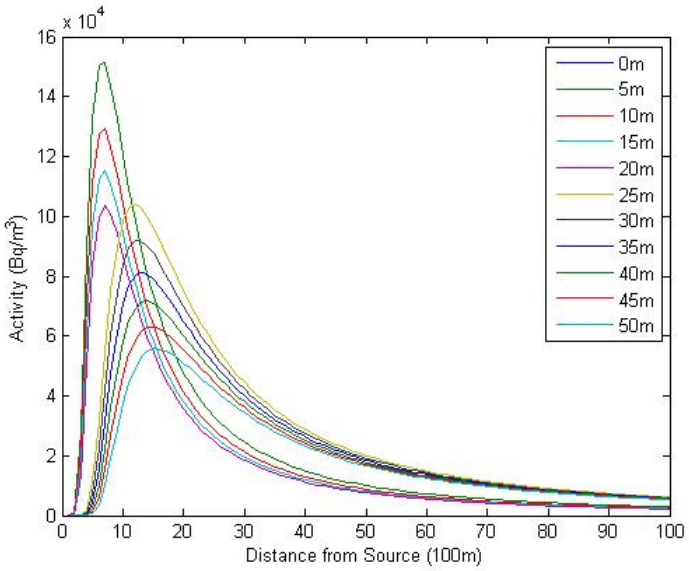

Figure 25: Stack Height Investigation

7.2. Isotope Separations Scenarios

7.2.1. 2.0 Ci/year Release Rate

The first scenario considers a source release rate of 2.0 Ci/year (63nCi/second). The minimum detectability limits for this activity is $0.0156\frac{\mu Ci}{m^3}$ for Xe-133 and $0.0811\frac{\mu Ci}{m^3}$ for Xe-135[33]. Table 9 shows all of the detection probabilities for all 10 different runs utilizing 1000

plumes simulated for both isotopes of radioxenon of interest. Furthermore, Table 9 depicts the mean and the standard deviation of these simulations.

Table 9: Detection Probability for 10 Trials (63 nCi/sec)

Run	Detection Probability (Xe-133)	Detection Probability (Xe-135)
1	100.00%	64.50%
2	100.00%	65.40%
3	99.80%	66.90%
4	99.70%	64.10%
5	99.80%	63.50%
6	99.90%	66.60%
7	100.00%	63.30%
8	100.00%	66.30%
9	99.90%	64.90%
10	100.00%	65.20%
Mean	99.91%	65.07%
σ	0.11%	1.26%

As calculated through Equation 6, the plume centerline was the area of highest concentration as the plume dispersed. Figure 26 shows the centerline activity in comparison with both MDAs for Xe-133 and Xe-135. As seen in Figure 26, the plume lies well above the line for the entire x axis (up to 10km) for Xe-133. Conversely, the Xe-135 MDA limits crosses the plume centerline at around 4.75 km. Figure 26 was compared to a graph of the detection probability as a function of the distance from the source, displayed in Figure 27. These two graphs differ significantly because Figure 27 indicates a detection probability much lower than the threshold at this distance

(approximately 10%). The detection probability as a function of distance reaches the 30% threshold at a distance of 8 km for Xe-133 and at a distance of 3.5 km for Xe-135 due to the randomized sampling of the environmental parameters. Variation in wind speeds were accounted for through the wind speed PDF. The detection level did not fall to critical levels for Xe-133 due to simulation limitations, though the detection level for Xe-135 fell to a few percent in about 4 km.

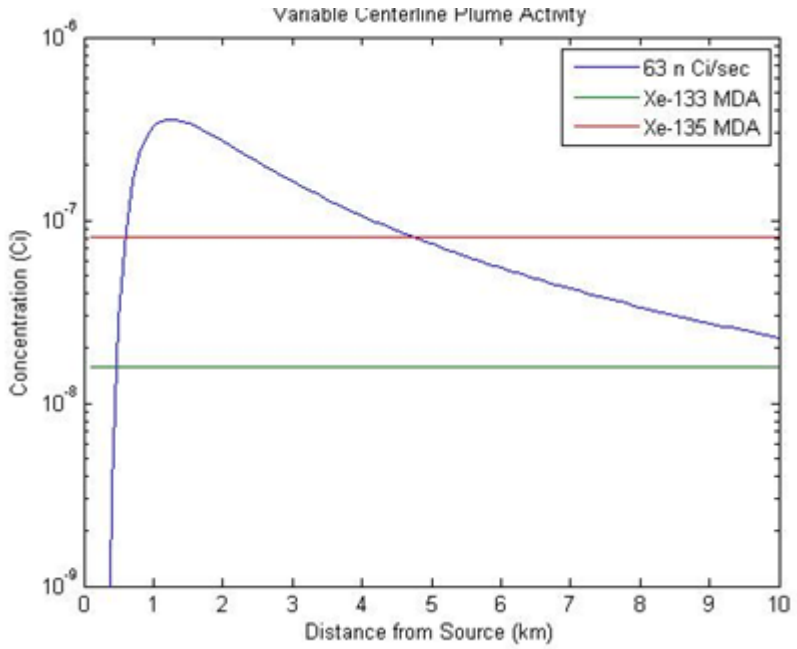

Figure 26: 2.0 Ci/year Plume Centerline using Xe-133 and Xe-135 (wind speed of 5 m/s)

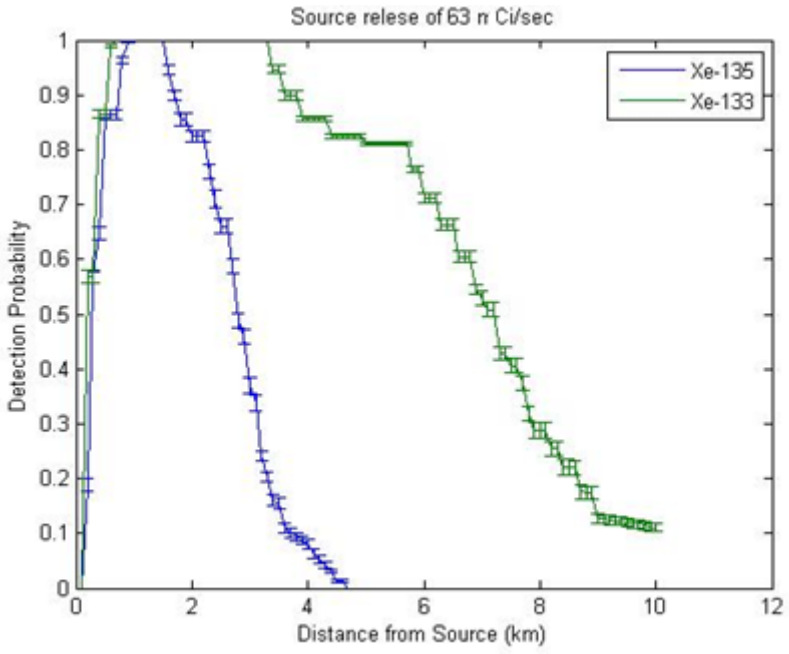

Figure 27: Detection Probability as a function of distance from the source with error bars

7.2.2. 1.6 Ci/year Release Rate

The second scenario considers a source release rate of 1.6 Ci/year (50 nCi per second). The minimum detectability limits for this activity is $0.0156\frac{\mu Ci}{m^3}$ for Xe-133 and $0.0811\frac{\mu Ci}{m^3}$ for Xe-135 [33]. Table 10 shows all of the detection probabilities for all 10 different runs utilizing 1000 plumes simulated for both radioisotopes of radioxenon. Furthermore, Table 10 depicts the mean and the standard deviation of these simulations.

Table 10: Detection Probability for 10 Trials (50 nCi/sec)

Run	Detection Probability (Xe-133)	Detection Probability (Xe-135)
1	99.90%	54.40%
2	99.60%	54.00%
3	99.80%	54.50%
4	99.70%	53.00%

5	99.90%	51.20%
6	99.70%	51.50%
7	99.40%	52.00%
8	99.70%	52.70%
9	99.60%	54.70%
10	100.00%	58.00%
Mean	99.73%	53.60%
σ	0.18%	2.00%

As calculated through Equation 6, the plume centerline was the area of highest concentration as the plume dispersed. Figure 28 shows the centerline activity in comparison with both of the MDAs. As seen in Figure 28, the plume lies well above the line for the entire x axis (up to 10km) for Xe-133 and the plume intersects the Xe-135 MDA at 3.75 km. Figure 28 was compared to a graph of the detection probability as a function of the distance from the source, displayed in Figure 29. These two graphs significantly because Figure 29indicates a detection probability much lower than the threshold at this distance (approximately 10%). The detection probability as a function of distance reaches the 30% threshold at around a distance of 7.5 km for Xe-133 and 2.75 km for Xe-135 due to the randomized sampling of the environmental parameters. Variation in wind speeds were accounted for through the wind speed PDF. The detection level did not fall to critical levels for Xe-133 at about 10 km, though the detection level for Xe-135 fell to a few percent at 3.75 km.

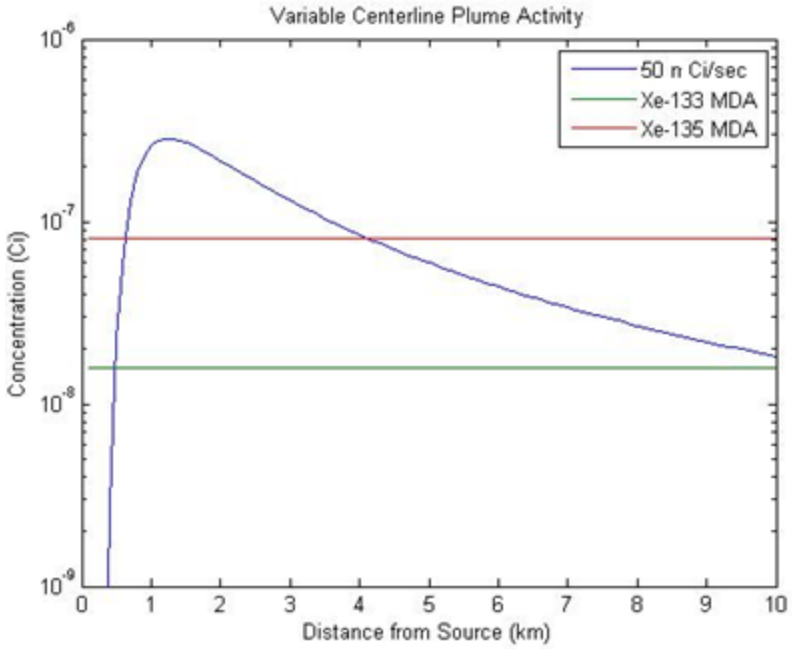

Figure 28: 1.6 Ci/year Plume Centerline using Xe-133 and Xe-135 (wind speed of 5 m/s)

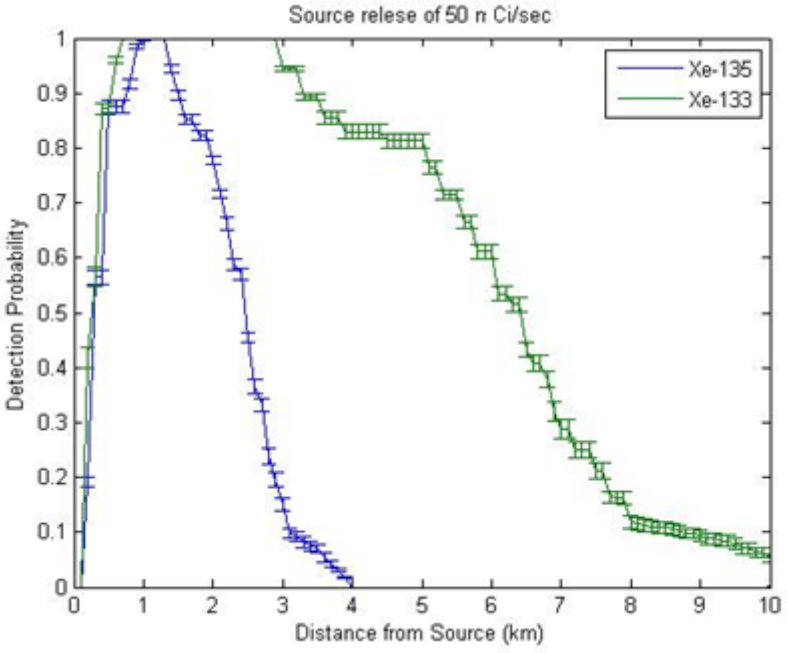

Figure 29: Detection Probability as a function of distance from the source with error bars

7.2.3. 1.2 Ci/year Release Rate

The third scenario considers a source release rate of 1.2 Ci/year (38 nCi per second). The minimum detectability limits for this activity is $0.0156\frac{\mu Ci}{m^3}$ for Xe-133 and $0.0811\frac{\mu Ci}{m^3}$ for Xe-135 [33]. Table 11 shows all of the detection probabilities for all 10 different runs utilizing 1000 plumes simulated for both isotopes of radioxenon. Furthermore, Table 11 depicts the mean and the standard deviation of these simulations.

Table 11: Detection Probability for 10 Trials (38 nCi/sec)

Run	Detection Probability (Xe-133)	Detection Probability (Xe-135)
1	99.50%	39.40%
2	99.70%	39.70%
3	99.40%	38.20%
4	99.30%	38.60%
5	99.40%	37.70%
6	99.20%	39.50%
7	99.40%	39.70%
8	99.20%	35.40%
9	98.60%	38.50%
10	99.40%	38.70%
Mean	99.31%	38.54%
σ	0.29%	1.29%

As calculated through Equation 6, the plume centerline was the area of highest concentration as the plume dispersed. Figure 30 shows the centerline activity in comparison with the MDAs of

each radioxenon isotope. As seen in Figure 30, the plume concentration intersects with the MDA at a distance of 9.25 km for Xe-133 and a distance of 3.25 km for Xe-135. Figure 30 compares this to a graph of the detection probability as a function of the distance from the source, displayed in Figure 31. These two graphs differ because Figure 31 indicates a detection probability much lower than the threshold at this distance (approximately 5%). The detection probability as a function of distance reaches the 30% threshold at around a distance of 6 km for Xe-133 and 2.25 km for Xe-135 due to the randomized sampling of the environmental parameters. Variation in wind speeds were accounted for through the wind speed PDF. The detection level did not fall to critical levels until about 9 kilometers for Xe-133 and 3.25 km for Xe-135, at which it fell to a few percent.

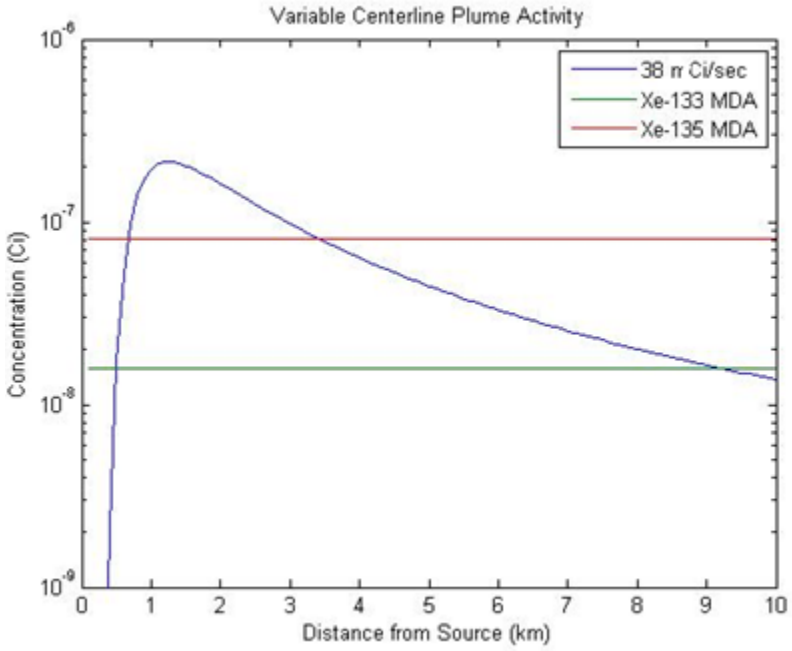

Figure 30: 1.2 Ci/year Plume Centerline using Xe-133 and Xe-135 (wind speed of 5 m/s)

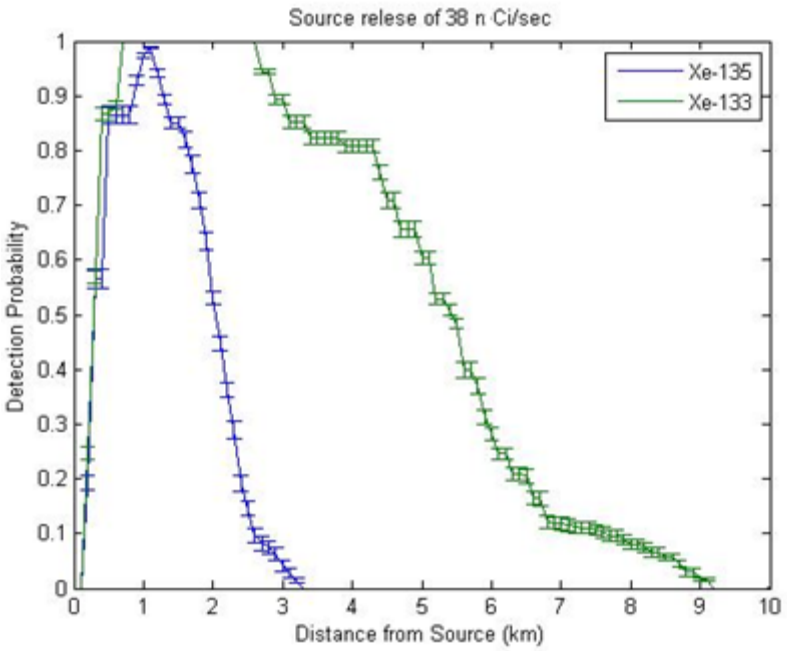

Figure 31: Detection Probability as a function of distance from the source with error bars

7.2.4. 0.8 Ci/year Release Rate

The fourth scenario considers a source release rate of 0.8 Ci/ year (25 nCi per second). The minimum detectability limits for this activity is $0.0156\frac{\mu Ci}{m^3}$ for Xe-133 and $0.0811\frac{\mu Ci}{m^3}$ for Xe-135 [33]. Table 12 shows all of the detection probabilities for all 10 different runs utilizing 1000 plumes simulated for both isotopes of radioxenon. Furthermore, Table 12 depicts the mean and the standard deviation of these simulations.

Table 12: Detection Probability for 10 Trials (25 nCi/sec)

Run	Detection Probability (Xe-133)	Detection Probability (Xe-135)
1	95.00%	20.10%
2	96.50%	20.50%
3	93.30%	19.20%

4	95.00%	22.50%
5	93.80%	21.50%
6	95.40%	21.80%
7	94.60%	21.10%
8	94.50%	22.30%
9	93.70%	19.80%
10	94.90%	23.00%
Mean	94.67%	21.18%
σ	0.93%	1.26%

As calculated through Equation 6, the plume centerline was the area of highest concentration as the plume dispersed. Figure 32 shows the centerline activity in comparison with the MDA. As seen in Figure 32, the plume intersects with the MDA at around 7.5 km for Xe-133 and 2.5 km for Xe-135. Figure 32 was compared to a graph of the detection probability as a function of the distance from the source, displayed in Figure 33. These two graphs differ because Figure 33 indicates a detection probability much lower than the threshold at this distance (a few percent). The detection probability as a function of distance reaches the 30% threshold at around a distance of 5 km for Xe-133 and 1.75 km for Xe-135 due to the randomized sampling of the environmental parameters. Variation in wind speeds were accounted for through the wind speed PDF. The detection level did not fall to critical levels until about 7 kilometers for Xe-133 and 2 km for Xe-135, at which it fell to a few percent.

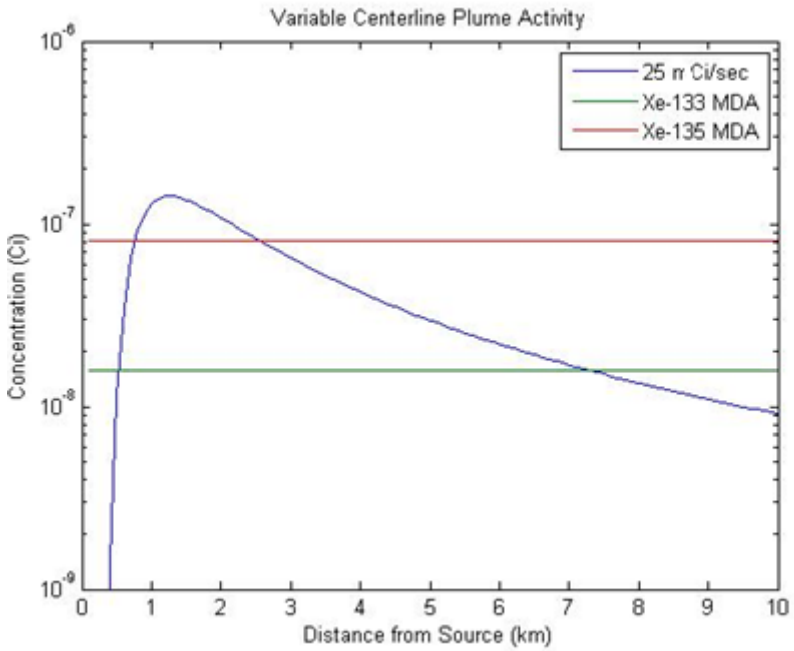

Figure 32: 0.8 Ci/year Plume Centerline using Xe-133 and Xe-135 (wind speed of 5 m/s)

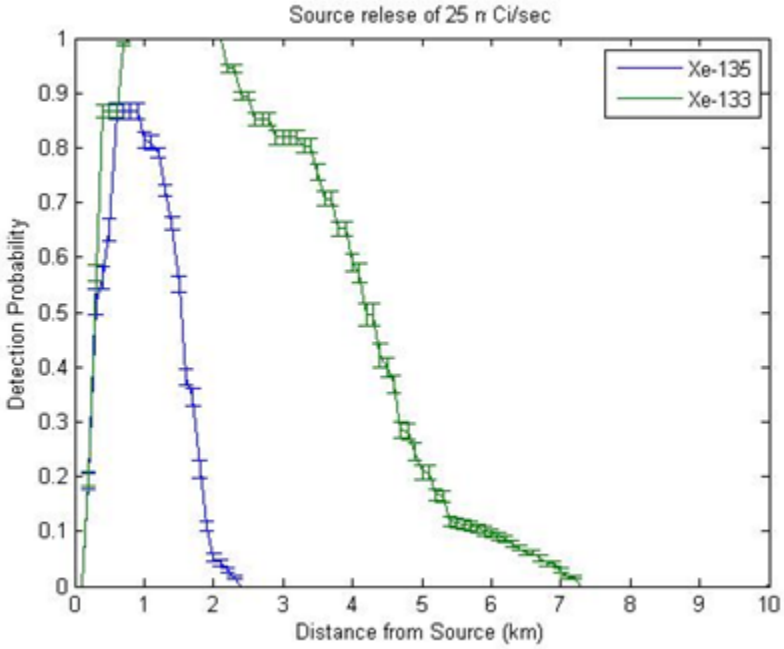

Figure 33: Detection Probability as a function of distance from the source with error bars

7.2.5. 0.4 Ci/year Release Rate

The final scenario considers a source release rate of 0.4 Ci/ year (12 nCi per second). The minimum detectability limits for this activity is $0.0156\frac{\mu Ci}{m^3}$ for Xe-133 and $0.0811\frac{\mu Ci}{m^3}$ for Xe-135 [33]. Table 13 shows all of the detection probabilities for all 10 different runs utilizing 1000 plumes simulated for both radioisotopes. Furthermore, Table 13 depicts the mean and the standard deviation of these simulations.

Table 13: Detection Probability for 10 Trials (12 nCi/sec)

Run	Detection Probability (Xe-133)	Detection Probability (Xe-135)
1	70.10%	1.50%
2	69.20%	2.30%
3	67.50%	2.70%
4	66.90%	2.60%
5	67.80%	2.10%
6	66.00%	2.10%
7	68.70%	2.80%
8	67.80%	2.80%
9	68.90%	2.80%
10	72.30%	2.80%
Mean	68.52%	2.45%
σ	1.78%	0.44%

As calculated through Equation 6, the plume centerline was the area of highest concentration as the plume dispersed. Figure 34 shows the centerline activity in comparison with both MDAs of

radioisotopes. As seen in Figure 34, the plume intersects with the MDA at around 4.75 km for Xe-133. However, the plume centerline does not cross the MDA of Xe-135. Figure 34 was compared to a graph of the detection probability as a function of the distance from the source, displayed in Figure 35. These two graphs differ as Figure 35 indicates a detection probability much lower than the threshold at this distance (a few percent). The detection probability as a function of distance reaches the 30% threshold at around a distance of 3.5 km for Xe-133 and 1 km for Xe-135 due to the randomized sampling of the environmental parameters. Variation in wind speeds were accounted for through the wind speed PDF. The detection level did not fall to critical levels until about 4.75 kilometers for Xe-133 and 1.25 km for Xe-135, at which it fell to a few percent.

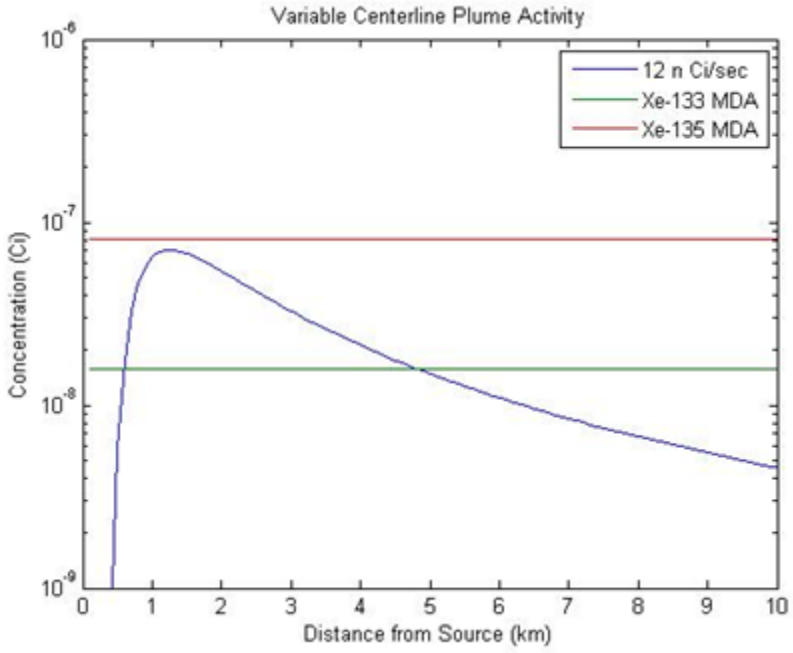

Figure 34: 0.4 Ci/year Plume Centerline using Xe-133 and Xe-135 (wind speed of 5 m/s)

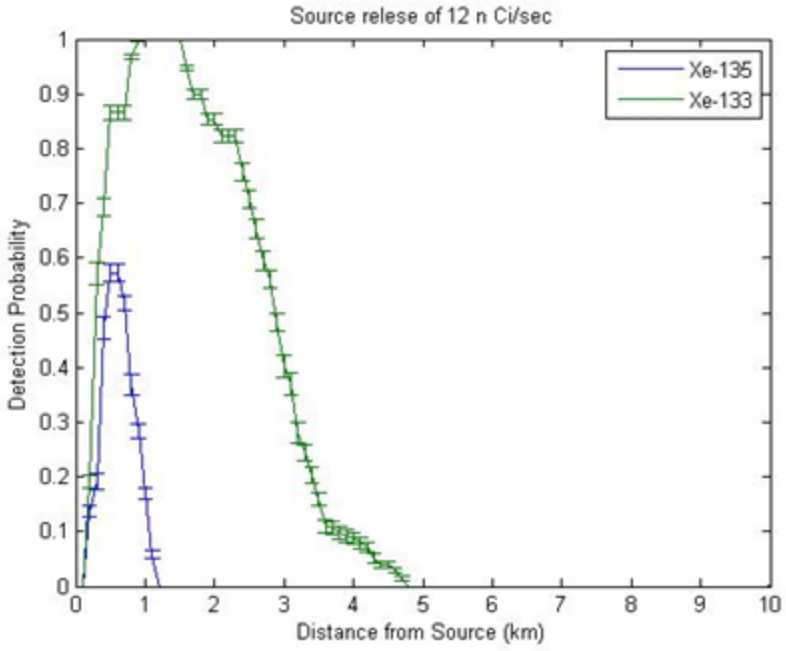

Figure 35: Detection Probability as a function of distance from the source with error bars

7.3. Detection Summary

For a proper understanding of the detection probability as a function of source release rate, a continuous distribution was required in order to view the overall trend. To obtain this distribution, runs were conducted all the way from 0.01 Ci/year to 2.0 Ci/ year in steps of 0.01 Ci/year. Furthermore, for each step, 10 separate simulations were conducted (each with 1,000 plumes) for both Xe-133 and Xe-135, providing assurance for each data point and allowed the continuous distribution, in Figure 36, to be compared with the error bar distribution, illustrated in Figure 37. This comparison ensured that the trend was supplemented with proper error consideration. Lastly, this detection probability was supported by comparing all of the plume centerline concentrations. As the material processing aggression increased, the concentration above both MDA limits occurred much farther away from the source, displayed in Figure 38.

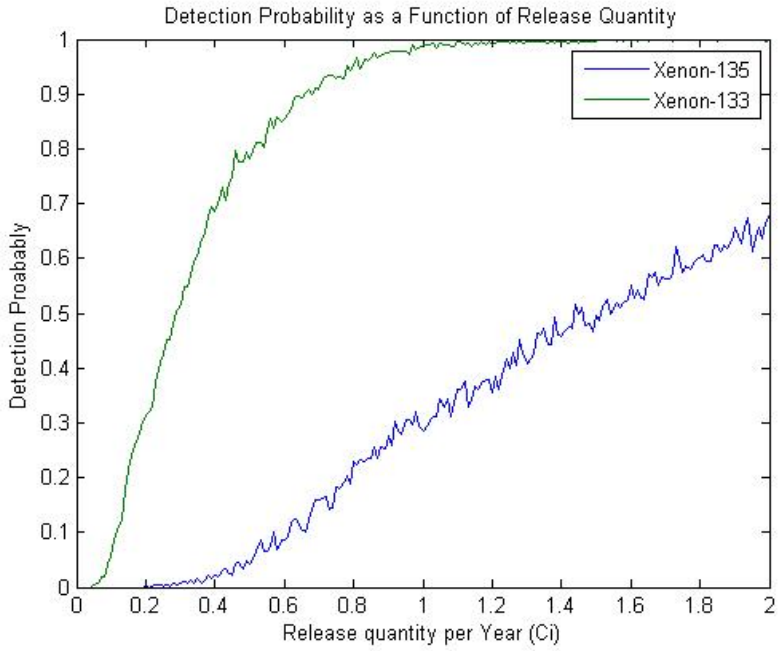

Figure 36: Detection Probability

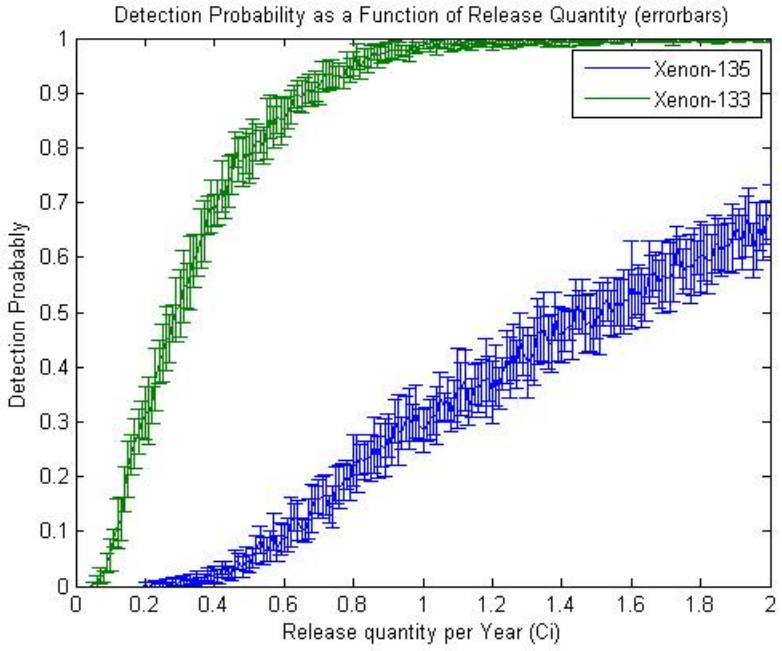

Figure 37: Detection Simulation Error Analysis

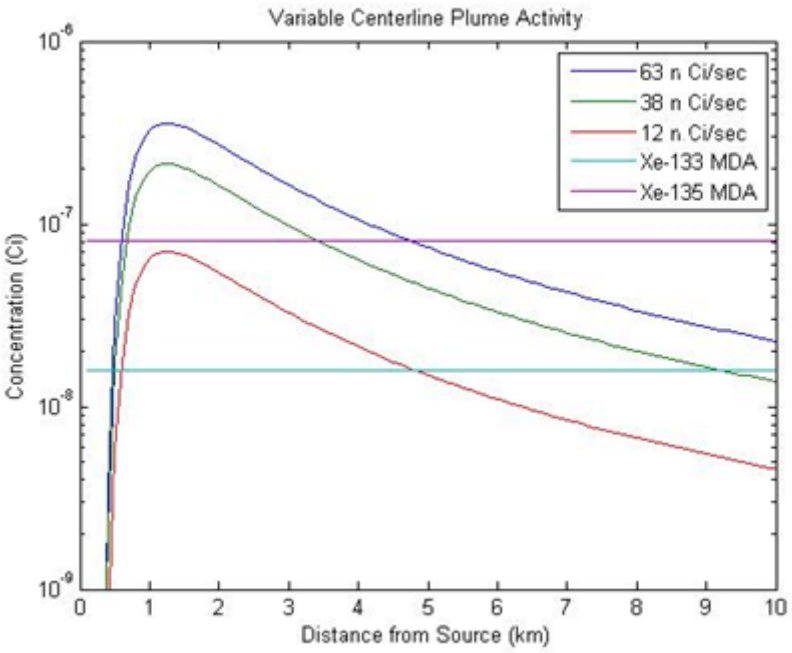

Figure 38: Plume Centerline Comparison

7.4. Probability of Detection

All of the previous simulations within this section have been relying upon the resulting number that indicates the probability of detection. However, investigation into thresholds of deterrence was required. A 100% detection rate would be convenient; this result is not achievable from a realistic or technical standpoint. When investigating a table of consequence versus likelihood, Figure 39 indicates five classes that identify the significance of potential consequences (1- no consequence and 5-severe consequence) associated with each root cause [66]. For the purposes of this situation, a consequence of 5 indicated the consequence for detection.

The next variable of interest was the likelihood of detection, which determined the root cause risk. The likelihood was determined through each set of individual simulation circumstances. However, the threshold of detection probability to ensure deterrence is still unknown, which relies heavily upon several factors that are a function of the area of which the isotope separation is taking place, the person or group separating the medical isotope, and the purposes behind the material production. Subsequently, this presents an in-depth philosophical

and psychological challenge, and was not considered within the scope of this thesis. However, after consulting the risk matrix, shown in Figure 39, there were two situations under consequence level 5 that yield a risk less than ‘high’ (red), which possessed a resulting likelihood of Low and Not Likely. Furthermore, Figure 40 elaborates on what the exact thresholds were for these two likelihoods. Since the largest probability of occurrence was 30%, this value was established as the threshold of deterrence when investigating the probability of detection.

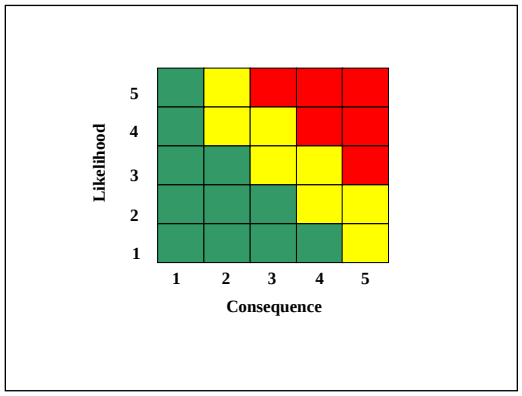

Figure 39: Action vs Consequence of Action [66]

Likelihood

Level	Likelihood	Probability of Occurrence
1	Not Likely	~10%
2	Low Likelihood	~30%
3	Likely	~50%
4	Highly Likely	~70%
5	Near Certainty	~90%

Figure 40: Likelihood Thresholds [66]

8. Analysis

With the understanding that 30% detection probability was the desired amount to provide adequate detection chance, this value can be applied back to medical isotope separation summary section. Figure 37 provides the most applicable information when using this threshold since it provided the continuous distribution of probability of detection versus material production capabilities. Applying the 30% threshold to Figure 37 results in an associated source release rate of 0.25 Ci per year for Xe-133 and a source release rate of 1 Ci per year for Xe-135, an expected trend considering the MDA for Xe-133 is much lower than the MDA for xenon-135. In fact, the MDA is about 5.17 times larger for Xe-135. Therefore, the detection distance does not scale linearly with MDA. When comparing this with previous studies conducted at PNNL, a desirable amount of 10^9 Bq/day is desirable but a release quantity of $5 * 10^9$ Bq/day is realistically achievable and desirable. When comparing this value to Figure 36, the values correspond to the

release rate of 9.8 Ci/year and 49 Ci/year. These values are well above the minimum detectable limits and would most certainly be detected at distances greater than 10 km. This claim is supported through as the atmospheric distributions of the 9.8 and 49 Ci/day release rates are represented through PNNL studies, with the dispersion concentrations as a function of release rate is shown in Figure 41.

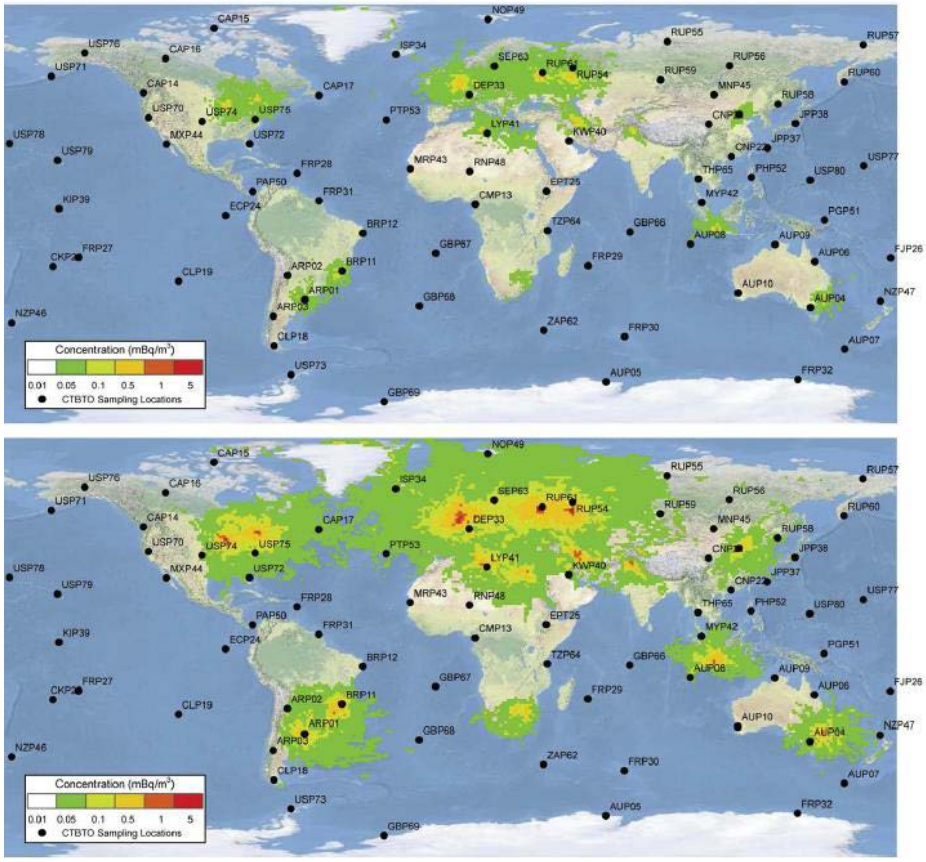

Figure 41: Dispersion Concentrations as a function of release rate [32]

This can also be applied to each individual circumstance in understanding the maximum distance away from the source in which a processing facility can be detected for each material production rate for the five scenarios. The results for the specific scenarios are depicted in Table 14. The continuous plot representing the minimum detectible distance as a function of material processing rate is depicted in Figure 42.

Table 14: Maximum Distance from Facility to achieve 30% Detection Probability

Scenario	Maximum Distance From Source (Xe-133)	Maximum Distance From Source (Xe-135)
2.0 Ci/year	7,850 meters	3,130 meters
1.6 Ci/year	7,130 meters	2,740 meters
1.2 Ci/year	6,060 meters	2,290 meters
0.8 Ci/year	4,690 meters	1,730 meters
0.4 Ci/year	3,190 meters	880 meters

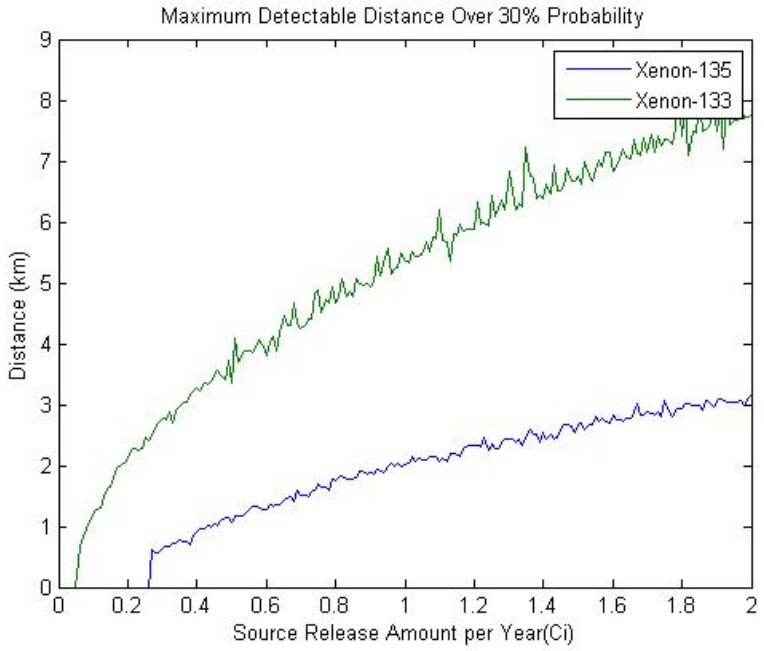

Figure 42: Maximum Detectable Distance to Yield Detection Probability Over 30%

9. Conclusion

As the states of the CTBT move forward with medical isotope production, it is a necessity to assure that monitoring methods of the CTBTO are maintained to be as effective as possible. One of the most important surveying methods is radionuclide detection for radioxenon isotopes. For this research, radionuclide detection was utilized for a medical facility through environmental sampling through the use of ^{133}Xe and ^{135}Xe detection. These radionuclides have different detection limits and thus will yield different detection rates due to the specific properties of the two isotopes. In order to ensure that the CTBTO technology maintains it capabilities, knowledge of the medical isotope facilities as well as their releases into the environment is of upmost importance. The releases from these facilities will cause background levels to rise, thus desensitizing the equipment utilized by the CTBTO to detect a nuclear detonation.

When creating several varying plume sources, the probability of detecting the source on a spatial mesh varies as a function of the source strength. Furthermore, as the source strength decreases, so does the detection probability, as shown in Figure 36. When the source strength level drops below a given threshold, this will result in a detection probability that will not provide adequate deterrence. The deterrence threshold is established through comparison of the risk versus the consequence of the facility being discovered. Through risk analysis, the threshold percentage occurs at a detection probability of 30%, with this value applied to the function relating material processing rate and the probability of detection.

A medical isotope production facility could be detected through the release of characteristic radioisotopes. The material processing rate reached the 30% detection probability at an associated production rate of 0.25 Ci per year for Xe-133 and 1.0 Ci per year for Xe-135. This is associated with an MDA of 0.58 $\frac{mBq}{m^3}$ for ^{133}Xe and 3 $\frac{mBq}{m^3}$ for ^{135}Xe.

Future studies pertaining to the detection of medical isotope facilities through environmental sampling could extend to case specific investigations. This study was intended to be a generic analysis (population density, environmental conditions, and uniform location meshing). However, tailoring these parameters to a specific situation could yield valuable and relevant information to current events. Furthermore, it could enable a more effective analysis of

the locations to determine where a medical isotope facility could operate with the lowest detection probability.

10.Bibliography

[1] M.-S. Yim and L. Jun, "Examining Relationship between Nuclear Proliferation and Civilian Nuclear Power Development.," *Progress in Nuclear Energy,* pp. 108-117, 2013.

[2] J. Li, Y. Man-Sung and D. McNeils, "Model-based Calculations of the Probability of a Country's Nuclear Proliferation Decisions," *Progress in Nuclear Energy,* 2010.

[3] International Atomic Energy Agency, "Information Circular 540," Decmenber 1 1998.

[4] N. Otsuka, "More efficient integrated safeguards by applying a reasonable detection probability for maintaining low presence probability of undetected nuclear proliferating activities," *Annals of Nuclear Energy,* 2013.

[5] M. Yue, L. Cheng and R. Bari, "Modeling and Evaluating Proliferation Resistance of Nuclear Energy Systems for Strategy Switching Proliferation," *Annals of Nuclear Energy,* pp. 11-26, 2013.

[6] S. Jacobsson, S. Grape, C. Hellesen and M. Lindell, "New Perspectives on Nuclear Power—Generation IV Nuclear Energy Systems to Strengthen Nuclear Non-proliferation and Support Nuclear Disarmament," *Energy Policy,* pp. 815-819, 2014.

[7] W. Lanham and T. Runion, "PUREX Process for Plutonium and Uranium Recovery," Oak Ridge National Laboratories, 1949.

[8] J. Flanary, S. Canster, R. Folger, J. Line, V. Reilly, V. Ryan and E. Sheldon , "Progress Report: PUREX Process," Oak Ridge, 1952.

[9] K. Williams, "A History of the U.S. Enrichment in the 1950s," *Oak Ridge National Laboratory,* 2004.

[10] W. Carr, S. Mann and B. Moncreif, "Uranium-Zirconium Alloy Fuel Processing in the ORNL Volatility Pilot Plant," AIChE Symposium, 1961.

[11] D. Olander, "Nuclear Fuel: Present and Future," *University of California, Berkely, Engineering Journal,* pp. 1-28, 2009.

[12] P. Dey, M. Giroux, A. Khaperskaya, J. Laidler, A. Machiels, M. Masson, F. Storrer and G. Uchiyama, "Spent Fuel Reprocessing Options," International Atomic Energy Agency, 2008.

[13] R. Taleyarkham, J. Lapinskas, B. Archhambault, J. Webster, T. Grimes, A. Hagen, K. Fisher, S. McDeavitt and W. Charlton, "Real-time Monitoring of Actinides in Chemical Nuclear Fuel Reprocessing Plants," *Chemical Engineering Research and Design*, pp. 688-702, 2013.

[14] B. Micklich, D. Smith, T. Massey, C. Fink and D. Ingram, "FIGARO: detecting nuclear materials using high-energy gamma rays," *Nuclear Instruments and Methods in Physics Research Section A: Accelerators, Spectrometers, Detectors and Associated Equipment* , pp. 466-469, 2003.

[15] J. Haire, "Nuclear Fuel Reprocessing Costs," *American Nuclear Society Topical Meeting,* 2003.

[16] M. Simpson and J. Law, "Nuclear Fuel Reprocessing," Idaho National Labs, 2010.

[17] J. Figueroa, M. Williamson, M. Van Kleek, R. Balaskovitz, T. Cruse, J. Willit, S. Chermerisov and G. Vandergrift, "GTRI Progress in Developing Pyrochemical processing for recovery of fabrication scrap and reprocessing of monolithic U-Mo Fuel," Argonne National Laboratory, 2011.

[18] I. Yasuhuito, T. Miyao, H. Sartorius, W. Weiss, K. Fushimi, M. Aoyama, K. Hirose and H. Inoue, "Kr-85 and Xe-133 monitoring at MRI, Tsukuba and its importance," *Journal of Environmental Radioactivity,* pp. 191-202, 2000.

[19] H. Daerr, M. Kalinowski, M. Kohler and P. Sahling, "Ultra-Trace Analysis of Kr-85," International Atomic Energy Agency, 2010.

[20] J. Hill, "Uranium Enrichment in the United States," *International Conference on Uranium Isotope Separation,* 1975.

[21] R. Smith, "The History of the Calutron," *A Historical Perspective,* 2005.

[22] G. U. i. t. U. States, S. Squassoni, S. Cooke, R. Kim and J. Greenberg, Governing Uranium in the United States, Washington: Rowman & Littlefield, 2014.

[23] US Department of Energy, "DOE Order-474.2 Nuclear Materials Control and Accountability," 2011.

[24] M. Laughter, "Prolifer of World Uranium Enrichment Programs," *Oak Ridge National Lab,* 2007.

[25] F. Kawakami, M. Tokiwai and Y. Fuji, "Plant designing of ion exchange chemical uranium enrichment and its non-proliferation aspects," *Progress in Nuclear Energy,* pp. 974-979, 2011.

[26] A. Glaser, "Detection of Special Nuclear Materials," Princeton Unviersity, 2007.

[27] J. Warner, K. Fitzsimmons, E. Reynolds, L. Gladkis and H. Timmer, "Exploration of Activity Measurements and Equilibrium Check for Sediment Dating Using Thick-Window Germanium Detectors," School of Physical, Environmental and Mathematical Science, University of New South Wales at the Australian Defense Academy, 2011.

[28] R. Korob and G. Nuno, "A simple method for the absolute determination of uranium enrichment by high-resolution γ spectrometry," *Applied Radiation and Isotopes,* pp. 525-531, 2006.

[29] H. Yucel and H. Dikmen, "Uranium enrichment measurements using the intensity ratios of self-fluorescence X-rays to 92* keV gamma ray in UXKα spectral region," *Talanta,* pp. 410-417, 2009.

[30] B. Boyer, "IAEA Verifications at an Uranium Erichment Plant," *Los Alamos national Labs.* , 2008.

[31] United Nations, "Comprehensive Test Ban Treaty," 1996.

[32] T. Bowyer, "Emissions from Fission-Based Medical Isotope Production and the Effects on the Internional Monitoring System," *Pacific Northwest National Labs,* 2015.

[33] P. Dresel and S. Waichler, "Evaluation of Xenon Gas Detection as a Means for Identifying Buried Transuranic Waste at the Radioactive Waste Management Complex, Idaho National Environmental and Engineering Laboratory," *Pacific Northwest National Labs,* 2004.

[34] M. Kalinowski, "Detection of Undeclared Reprocessing," *APS Verification Study,* 2009.

[35] M. Schoopner, "Analysis of Glocal Radioxenon Background with Atmospheric Transport Modeling for Nuclear Explosion Monitoring," *University of Roma Tre Department of Physics,* 2012.

[36] D. Fisher, "Medical Isotope Production and Use," *PNNL-SA-65456,* 2009.

[37] T. Holschuh, M. MacDougall, W. Moore and K. Zieb, "Estimation of Nuclear Proliferation Capacity of Test Reactors in Mink," *Oregon State University,* 2013.

[38] S. Henderson, J. Holmes and Y. Zhang, "Introduction fo Accelerators," USPAS, 2009.

[39] C. Liu, "Nuclear Process and Raio-Analytical Chemistry," *Nuclear Engineer Divison of the American Instituation for Chemical Engineers,* p. Chemistry session 3.2.

[40] M. Simpson, "Developments of Spent Nuclear Fuel Pyroprocessing Technology at Idaho National Laboratory," Idaho National Labs, 2012.

[41] M. Williamson, "Pyroprocessing Technologies: Recycling Used Nuclear Fuel for a Sustainable Energy Future," *Argonne National Labs,* 2012.

[42] Los Alamos National Laboraty, "MCNP- A General Monte Carlo N-Particle Transport Code, Version 5," no. LA-UR-03-1987, April 24 2013.

[43] Comprehensive Test Ban Treaty Oranization, "Spectrum," *CTBTO Magazine,* vol. September 2013.

[44] T. Bowyer, "Xenon Monitoring and the Comprehensive Nuclear-Test-Ban Treaty," *Pacific Northwest National Lab,* no. PNNL-SA-98831.

[45] International Atomic Energy Agency, INFCIRC/140 Treaty on the Non-Proliferation of Nuclear Weapons, Vienna, Austria, 1970.

[46] International Atomic Energy Agency, "The Structure and Content of Agreements Between the Agency and States Required in Connection with the Treaty on the Non-Proliferation of Nuclear Weapons," *INFCIRC/153,* 1972.

[47] International Atomic Energy Agency, "Information Circulars," 2015. [Online]. Available: https://www.iaea.org/publications/documents/infcircs.

[48] International Atomic Energy Agency, "Inspection of Radiation Sources and Regulatory Enforcement," IAEA-TECDOC-1526, Vienna, Austria, April 2007.

[49] D. Donohue, "Tools for Nuclear Inspection," IAEA Information Series, Division of Public Information, 04-46161 FS Series 3/03/E, Vienna, Austria.

[50] D. Donohue, "Key Tools for Nuclear Inspections: Advances in Environmental Sampling Strengthen Safegaurds," Analytical Chemistry, Vol. 74, No. 1, International Atomic Energy Agency, Vienna, Austria.

[51] National Nuclear Security Administration, "Prevent, Counter, and Respond—A Strategic Plan to Reduce Global Nuclear Threats," 2014. [Online]. Available:

http://nnsa.energy.gov/aboutus/ourprograms/dnn/npcr.

[52] National Nuclear Security Administration, "Prevent, Counter, and Respond—A Strategic Plan to Reduce Global Nuclear Threats (FY 2016–FY 2020)," Department of Energy, Washington, DC, March 2015.

[53] Department of Energy, "Strategic Plan," Washington, DC, 2011.

[54] National Nuclear Security Administration, "NA-20 Organization Chart," Washington, DC, 2005.

[55] United Nations, "Security Resolution 1540," UN, April 2004.

[56] International Atomic Energy Agency, "Information Circular 209," IAEA, Vienna, Austria, June 2014.

[57] C. Walrond, *Timeline 1967-1993: Argentine Low-Enriched Uranium at Tehran Research REactor*, Institute for Science and International Security, 2009.

[58] United Nations, "Study on Israeli Nuclear Armament," *United Nations Centre for Disarmament*, 1982.

[59] Lawrence Berkely National Lab, "Fission Product Yeilds," *Isotopes Projects, Nuclear Science Divison*, 1998.

[60] J. Kaye and R. Warner, "Beta-Gated Gamma Coincidence Counting with a Phoswich Detector," *Pacific Northwest National Labs*, no. PNL-SA-9159.

[61] T. Heimbinger, T. Bowyer, J. McIntyre, K. Abel, J. Hayes, M. Panisko and W. Pitts, "The DOE Automated Radioxenon Sampler-Analyzer (ARSA) Beta-Gamma Coincidence Spectrometer Data Analyzer," *Pacific Northwest National Laboratory*, no. DE-AC06-76RLO 1830.

[62] M. Jordan and S. Jain, "Monte Carlo Sampling," *STAT-260*, 2010.

[63] M. Batty and P. Longley, "Form Folows Function: Reformulating Population Desntiy Functions," in *Fractal Cities*, San Diego, CA, Academic Press, INC., 1994, pp. 308-334.

[64] Allen and Durrenberger, "Gaussian Plume Modeling," *Chemical Engineering 357-University of Texas*.

[65] J. Hartman, J. Kelly and J. Birnbaum, "A case for Employing Near-field Measurments to Detect Important Effluents from Nuclear Material Process Operations," *Pacific Northwest National Labs Technical Documents,* 2007.

[66] Department of Defense, "Risk Management Guide for DOD Acquisition," *Sixth Edition,* 2008.

[67] W. Warburton, W. Henning, A. Fallu-Labuyere, K. Sabourov, M. Cooper, J. McIntyre, A. Gleyzer, M. Bean, E. Korpach, K. Ungar, W. Xahng, P. Mekarski, R. Ward, S. Biegalski and D. Haas, "RadioXenon Measurment with the Photoswatch Detector System," 2009.

[68] J. Waner, K. Fitzsimmons, E. Reynolds, L. Gladkis and H. Timmer, "Exploration of Activity Measurments and Equilibrium Check for Sedmiment Dating Using Thick-Window Germanium Detectors," *School of Physical, Environmental, and Mathmatical Science, University of New South Wales at the Australian Defesne Academy,* 2011.

[69] J. Rob, "Simulation of atmospheric Kr-85 transportation to access the detectibility of clandestine nuclear reprocessing," *Max-Plank Research School on Earch System Modeling,* 2010.

[70] D. Reiter, "Preventive Attacks Against Nuclear Programs and the “Success” at Osiraq," *Viewpoint,* 2010.

[71] W. Perry and C. Ferguson, "US Nuclear Weapons Policy," *US Nuclear Weapons Policy ,* 2009.

[72] A. Glaser, "Detection of Special Nuclear Material," *Princeton University,* 2007.

[73] A. Farsoni, D. Hamby, K. Ropon and S. Jones, "A two-channel photoswitch detector for dual and tripple coincidence measurements or radioxenon," *Proceedings of the 29th Monitoring Research Review: Ground-Based Nuclear Explosion Monitoring Technologies,* Vols. LA-UR-07-5613 Vol 2, pp. 747-756, 2007.

[74] M. Elleman, D. Esfandiary and E. Hokayem, "Syria’s Proliferation Challenge and the European Union’s Response," *EU Non-Proliferation Consortium,* 2012.

[75] T. Dokos, "Iran’s Nuclear Propensity: The Probability of Nuclear Use," *EU Non-Proliferation Consortium,* 2014.

[76] I. Adsley, A. L. Nichols and J. Toole, "Decay of Th-234 and Pa-234m in Secular Equibrium: Resolution of Observed Anomolies," *DOE/CPR2/41/1/219,* 1996.

[77] National Nuclear Security Administration, "Nonproliferation," 2015. [Online]. Available: http://nnsa.energy.gov/aboutus/ourprograms/nonproliferation-0.

[78] International Atomic Energy Agency, "IAEA Safegaurds Glossary," *International Nuclear Verification Series No. 3*, p. 23, 2001.

11. Appendix A- Derivations

11.1. Centerline maximum concentration location

$$\mathrm{X}(x) = \frac{Q}{\pi\sigma_y\sigma_z a}\exp\left(-\frac{1}{2}\left(\frac{H}{\sigma_z}\right)^2\right), \sigma_y = cx^d, \sigma_z = ax^b$$

$$X(x) = \frac{Q}{\pi c x^d a x^b}\exp\left(-\frac{1}{2}\left(\frac{H}{ax^b}\right)^2\right)$$

$$X(x) = \frac{Q}{\pi ca} * \frac{\exp\left(-\frac{1}{2}\left(\frac{H^2}{a^2x^{2b}}\right)\right)}{x^{d+b}}$$

$$\frac{D\mathrm{X}(x)}{dx} = \frac{Q}{\pi ca} * \frac{df(x)}{dx}, where \frac{\exp\left(-\frac{1}{2}\left(\frac{H^2}{a^2x^{2b}}\right)\right)}{x^{d+b}} = f(x)$$

$$\frac{df(x)}{dx} = \frac{d}{dx}\left(\exp\left(-\frac{H^2}{2a^2x^{2b}}\right) * x^{-(b+d)}\right)$$

$$\frac{df(x)}{dx} = \left[\exp\left(-\frac{H^2}{2a^2x^{2b}}\right) * \frac{H^2}{2ax^{2b}} * x^{-(d+b)}\right] + \left[\exp\left(-\frac{H^2}{2a^2x^{2b}}\right) * -(d+b)x^{(-d-b-1)}\right]$$

Setting the derivative equal to zero

$$0 = \frac{Q}{\pi ca} * \left[\exp\left(-\frac{H^2}{2a^2x^{2b}}\right) * \frac{H^2}{2ax^{2b}} * x^{-(d+b)}\right] + \left[\exp\left(-\frac{H^2}{2a^2x^{2b}}\right) * -(d+b)x^{(-d-b-1)}\right]$$

$$0 = \frac{H^2}{2a} * 2b\left(x^{-(2b+1)}\right) - (d+b)x^{-(d+b+1)}$$

$$\frac{H^2 b}{a(d+b)} = \frac{x^{-(d+b+1)}}{x^{-(2b+1)}}$$

$$\frac{H^2 b}{a(d+b)} = x^{d-b}$$

$$x_{max} = \frac{\log\left(\frac{H^2 b}{a(d+b)}\right)}{\log(d-b)}$$